Linking soil moisture content and carbon dioxide fluxes: From batch experiments to process-based modelling

by

Linden Grace Fairbairn

A thesis

presented to the University of Waterloo

in fulfilment of the

thesis requirement for the degree of

Master of Science

in

Earth Sciences (Water)

Waterloo, Ontario, Canada, 2020

Author's declaration

This thesis consists of material all of which I authored or co-authored: see Statement of Contributions included in the thesis. This is a true copy of the thesis, including any required final revisions, as accepted by my examiners.

I understand that my thesis may be made electronically available to the public.

Statement of contributions

Chapter 2 of this thesis consists of a co-authored, manuscript-format paper. As the first author, I was primarily responsible for the study design, execution, data collection and analysis, and writing. The contributions of the listed co-authors are as follows:

The experiment was designed by me with the guidance of Fereidoun Rezanezhad, Philippe Van Cappellen, Chris Parsons, and Merrin Macrae. All laboratory work was carried out by me, with the assistance of Marianne VanderGriendt, Senior Research Technician, for some analyses. Application of the numerical model was completed by Mehdi Gharasoo and myself. I wrote the manuscript which was subsequently reviewed by the co-authors.

I am the sole author of all other chapters in this thesis.

Abstract

The emissions of carbon dioxide (CO_2) from soil to the atmosphere represent a major flux within the global carbon cycle. Soil CO_2 fluxes depend on environmental factors including soil moisture and oxygen, and on intrinsic physical and chemical properties of the soil itself. The responses of soil CO_2 fluxes to changes in environmental conditions remain unclear but are critical for predictive modelling of carbon fluxes with climate change. The numerous processes involved in soil CO_2 production and some of their driving factors are reviewed and discussed in Chapter 1 of this thesis.

In Chapter 2, I examined the effects of both soil moisture and oxygen on soil CO_2 fluxes through experimentation and modelling. Soil moisture and oxygen are closely linked: given a constant pore volume, gas-filled pore space decreases as the proportion of water-filled pore space increases, both of which influence soil aerobic and anaerobic microbial processes. To decouple the effects of soil moisture and oxygen, I conducted a factorial batch experiment by incubating an agricultural soil collected from the field and adjusted to different moisture contents (30%-100% water-filled pore space; WFPS) and under oxic versus anoxic headspaces. Gas fluxes (CO_2 and methane) and pore water chemistry parameters were measured at the end of the 21-day incubation. The results demonstrated that, as expected, CO_2 fluxes became moisture-limited at low soil moisture and oxygen-limited at high soil moisture; hence, fluxes were maximal at moderate moisture content (65% WFPS). Non-zero and, at times, substantial fluxes at 100% saturation and under anoxic incubation demonstrated that anaerobic sources contributed to overall CO_2 fluxes in addition to aerobic respiration. CO_2 fluxes under anoxic headspaces were affected by soil moisture independently of oxygen availability, with maximum fluxes occurring at 100% saturation. At high moisture contents (80% and 100% WFPS), CO_2 fluxes in anoxic incubations were 75% to >100%

of those in oxic incubations. Methane fluxes, production of low molecular weight organic acids and depletion of other electron acceptors indicated that fermentation and methanogenesis were likely the main pathways for CO_2 production occurring at the end of the anoxic incubation. These results demonstrated that anaerobic production of CO_2 (via fermentation, methanogenesis and/or anaerobic respiration) can be an important source that has been ignored in existing models which typically only consider aerobic respiration. A simple formulation for incorporating anaerobic sources in existing models was developed. These results highlight that CO_2 is produced by a collection of soil processes and therefore model development needs to move beyond the simplified "soil respiration" representation and incorporate a process-based understanding of greenhouse gas-emitting processes in soil.

In Chapter 3, I reviewed the current state of knowledge regarding the effect of soil texture on soil CO_2 fluxes. While many past studies have investigated the protective effect of clay on soil organic matter, I focussed this discussion on the potential interaction between soil texture and soil moisture in controlling soil CO_2 fluxes. The review identified that, while some studies have developed a conceptual framework for making predictions about this possible interaction, very few studies have tested these predictions experimentally. As a first step in investigating soil texture and soil moisture in a factorial experiment, I conducted another batch experiment where I prepared three artificial soils of varying textures (ranging from approximately 7%-20% clay content) and incubated soil samples at different moisture contents (ranging from approximately 7%-100% WFPS). The measured CO_2 fluxes and their relationship with soil moisture were affected by soil texture, although the way in which soil moisture was expressed (gravimetric vs. % WFPS) affected the functional dependence of the CO_2 fluxes on soil texture. More direct experimental data and improvements to the experimental methods will be required to advance our process-based

understanding of how soil texture and soil moisture affect CO_2 fluxes. This process-based understanding is prerequisite to the development and validation of models that accurately represent these controlling factors.

Acknowledgements

Thank you to my supervisors, Philippe Van Cappellen and Fereidoun Rezanezhad, for your unwavering support and for the amazing opportunities I have received during my time with the Ecohydrology group. Thank you, Fereidoun, for believing in me since the beginning and for your encouragement even on the toughest days. Thank you, Philippe, for sharing your energy and passion for science with me and for always steering me in the right direction.

Thank you to Chris Parsons, for always being able to answer my questions about biogeochemistry, and about my future career direction – your advice has been so valuable to me. Thank you to Merrin Macrae, for all your thoughtful advice about my experiments. Thanks also to Thai Phan for agreeing to join my committee at the last minute and your thoughtful questions.

Many thanks to Marianne VanderGriendt, whose diligent training in the lab throughout my time with Ecohydrology is a major reason for the success of my Masters research. Thank you also to Amanda Niederkorn, who has answered so many of my questions in the lab.

This research would not have been possible without the support of our funding sources: an NSERC Strategic Partnership Grant (STPGP494652-16) and the Canada Excellence Research Chair program in Ecohydrology awarded to Philippe Van Cappellen. I have also been very fortunate to receive support from the following scholarships: Alexander Graham Bell Canada Graduate Scholarship (NSERC), Queen Elizabeth II Graduate Scholarship in Science and Technology (Government of Ontario), President's Scholarship (University of Waterloo), ***rare*** Ages Foundation Bursary (***rare*** Charitable Research Reserve), and a Canadian Water Resources Association Scholarship.

My thanks go to everyone in the Ecohydrology Research Group who taught me something in the lab, helped me interpret some weird results, or shared encouraging words with me. Thank you to Adrian, Christina, and Geertje for your guidance, to Steph and Tamara for your edits and your endless encouragement while I finished this thesis, and to Mehdi for your help with the modelling component of this Masters. Thank you to my fellow students over the years for sharing in the ups and downs with me: Danny, Tatjana, Heather, Konrad, Nady, Shengde, and so many others. Thanks also to the co-op students who helped in the lab, especially Kelly for her help with my final experiment.

Thank you to my parents, Rick and Barb, and my brother Jimmy, for always believing in me and sharing with me a curiosity and love of nature.

Finally, thank you to John, for being there with an encouraging thumbs up and smile during my presentations, making great dinners, picking me up from campus after long days, and always seeing the best in me even when I struggled most.

Table of contents

List of figures

List of tables

List of abbreviations

CO_2	Carbon dioxide
WFPS	Water-filled pore space
OM	Organic matter
C	Carbon
GHG	Greenhouse gas
O_2	Molecular oxygen
POC	Particulate organic carbon
DOC	Dissolved organic carbon
EA	Electron acceptor
N_2O	Nitrous oxide
CH_4	Methane
DIC	Dissolved inorganic carbon
EC	Electrical conductivity
IC	Ion chromatography
ATP	Adenosine triphosphate

List of symbols

θ	Volumetric water content	(cm^3 cm^{-3} soil)
ϕ	Porosity	(cm^3 cm^{-3} soil)
ρ_b	Bulk density	(g dry soil cm^{-3})
F_{gas}	Calculated gas flux	(nmol cm^{-3} soil hr^{-1} or µmol kg^{-1} dry soil hr^{-1})
ΔC_{gas}	Change in gas concentration (measured)	(µmol mol^{-1})
V	Headspace volume	(L)
R	Gas constant	(L atm K^{-1} mol^{-1})
T	Temperature	(K)
Δt	Duration of gas flux measurement	(hr)
v_{soil}	Volume of soil sample	(L)
m_{soil}	Dry mass of soil sample	(kg)
R_{CO2}	Modelled total CO_2 flux	(nmol cm^{-3} soil hr^{-1})
R_{Ox}	Modelled CO_2 flux from aerobic respiration	(nmol cm^{-3} soil hr^{-1})
R_{An}	Modelled CO_2 flux from combined anaerobic sources	(nmol cm^{-3} soil hr^{-1})
DOC_{av}	Available DOC concentration at the reaction site	(µmol cm^{-3} soil)
$[DOC]$	Concentration of DOC in the soil water	(µmol cm^{-3} soil)
$O_{2,liq}$	Available O_2 concentration at the reaction site	(µmol cm^{-3} soil)
n	Exponent relating DOC_{av} to moisture content	(dimensionless)

$V_{max,Ox}$	Maximum CO_2 flux from aerobic respiration	(nmol cm^{-3} soil hr^{-1})
$V_{max,An}$	Maximum CO_2 flux from anaerobic sources	(nmol cm^{-3} soil hr^{-1})
$k_{c,Ox}$	Half-saturation constant for DOC in oxic incubations	(µmol cm^{-3} soil)
$k_{c,An}$	Half-saturation constant for DOC in anoxic incubations	(µmol cm^{-3} soil)
k_o	Half-saturation constant for O_2	(µmol cm^{-3} soil)
k_{in}	Coefficient for O_2 inhibition of anaerobic CO_2 production	(µmol cm^{-3} soil)
θ_s	Relative saturation (WFPS)	(cm^3 cm^{-3} soil)
θ_r	Residual moisture content	(cm^3 cm^{-3} soil)
D_l	Diffusion coefficient for aqueous	(dimensionless)
D_g	Diffusion coefficient for gas	(dimensionless)
n_{Ox}	Value of exponent *n* in oxic incubations	(dimensionless)
n_{An}	Value of exponent *n* in anoxic incubations	(dimensionless)
$[DOC]_{Ox}$	DOC concentration in oxic incubation	(µmol cm^{-3} soil)
$[DOC]_{An}$	DOC concentration in anoxic incubation	(µmol cm^{-3} soil)
D_p/D_o	Relative gas diffusivity	(dimensionless)
$D_s/D_{o,s}$	Relative solute diffusivity	(dimensionless)
ε	Air-filled porosity	(cm^3 cm^{-3} soil)
θ_{th}	Threshold moisture content	(cm^3 cm^{-3} soil)
SA_{vol}	Volumetric soil surface area	(cm^2 cm^{-3} soil)

1 Introduction

1.1 Soils and the global carbon cycle

Soils represent the largest active terrestrial reservoir of carbon (C) on Earth, storing upwards of 2500 Pg of C in the uppermost 1 metre globally (Eswaran *et al.*, 1993). Approximately 1500 Pg of this soil C pool is made up of organic C from dead organic matter (OM) in varying degrees of decomposition in the soil and on the soil surface (estimates range from 504-3000 Pg, with a median of 1460.5 Pg; Lal, 2010; Scharlemann *et al.*, 2014). Carbon storage is a key function of soils and the potential for enhanced C sequestration in soils has received increasing attention (Wiesmeier *et al.*, 2014), especially for agricultural soils due to the historic depletion of organic C in cultivated lands (Lal, 2004; Smith, 2004). Soil OM is also an important indicator of soil health and fertility; therefore, stabilizing and maintaining soil OM is critical for food production – another key function of soils globally (Doran, 2002). Consequently, the importance of understanding the stability of soil organic C cannot be overstated.

The exchange of C between soils and the atmosphere represents an important flux in the global C cycle. The emission of carbon dioxide (CO_2), one form of inorganic carbon, results from the decomposition of organic C in soil. Decomposition of OM in soils is a major source of C to the atmosphere: global fluxes have been estimated at 75 Pg C yr^{-1} (Raich and Schlesinger, 1992; Raich and Potter, 1995), much larger than estimates of fossil fuel and cement emissions (9.5 Pg C yr^{-1} in 2010; Peters *et al.*, 2012). Losses of C as CO_2 from soil are largely balanced by CO_2 uptake via primary production, with terrestrial ecosystems estimated to be a slight net sink (Figure 1-1; Schimel, 1995; Berner and Berner, 2012) . However, due to the magnitude of the annual fluxes and relatively short residence time of C in soil, even minor perturbations to this balance could represent an impactful change to the size of the atmospheric C reservoir.

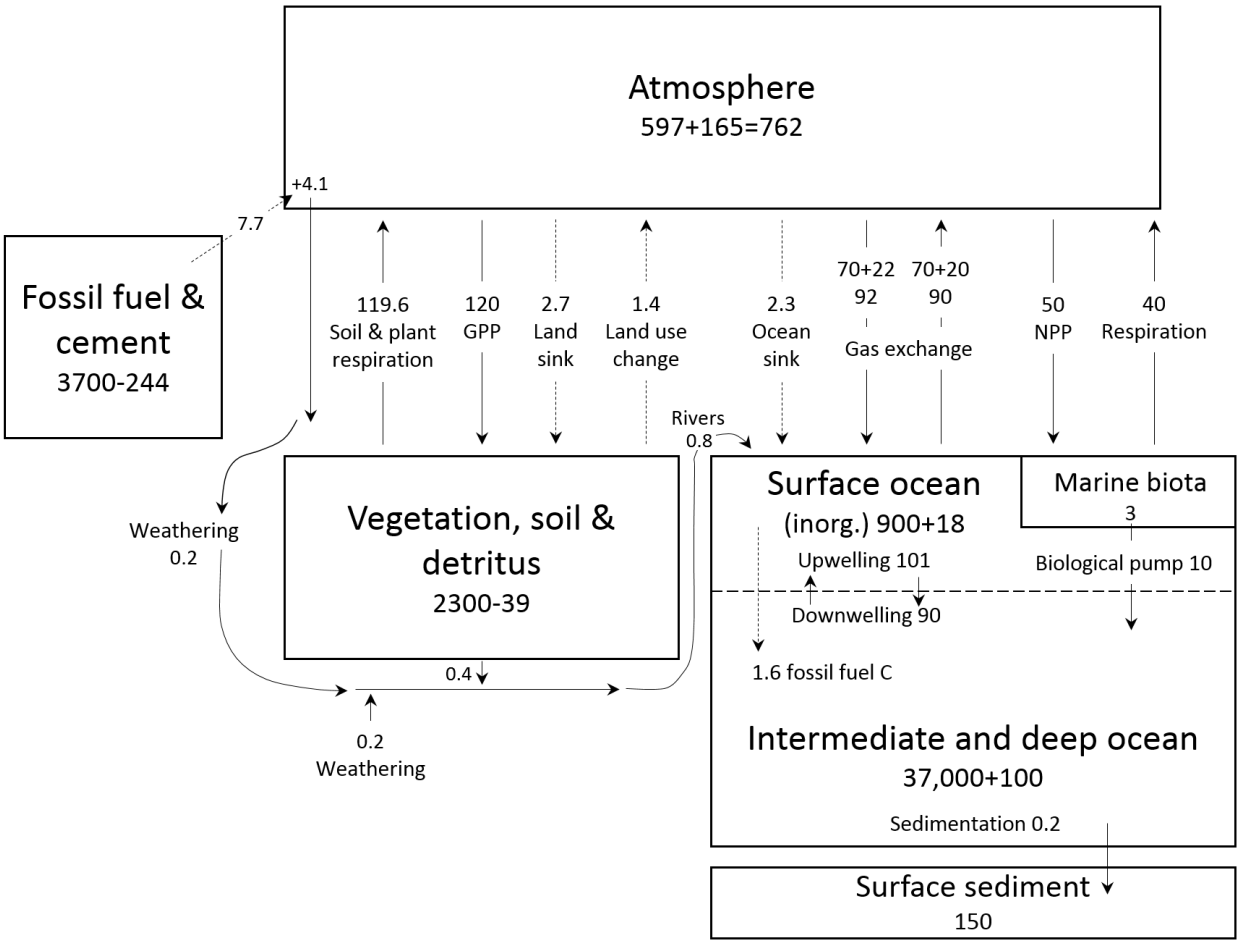

Figure 1-1: Box model diagram of the surficial carbon cycle (redrawn from Berner and Berner, 2012). Reservoir sizes are in Pg C, and fluxes are in Pg C yr^{-1}. Solid arrows represent "natural" fluxes while dashed arrows represent anthropogenic fluxes, and reservoir sizes are shown as the pre-anthropogenic size plus or minus the reservoir size change caused by humans. Note the closely balanced but large magnitude fluxes to and from the soil reservoir.

One obvious implication of any change in the size of the atmospheric CO_2 reservoir is its capacity to warm the planet through the greenhouse effect. The International Panel on Climate Change (IPCC) has reported that humans have already caused an increase in global temperatures of 1.0°C above pre-industrial levels and will likely reach 1.5°C by the years 2030-2052 (IPCC, 2018). On average, areas in Canada will continue to experience double the global increase in temperatures (Bush and Lemmen, 2019). Though emissions of CO_2 (and other greenhouse gases, such as methane and nitrous oxide) from soil might be considered as a "natural" process, anthropogenic activities impact the magnitude of these fluxes. For example, land management practices can affect rates of organic carbon turnover and nitrous oxide emissions from agricultural soils (Smith *et al.*, 2008). The effects of climate change may even result in accelerated greenhouse gas (GHG) emissions from soil, for example, due to elevated temperatures or changing precipitation regimes (Davidson and Janssens, 2006), which would present an alarming positive feedback mechanism for global warming. The IPCC has reported that increased CO_2 emissions from soils due to climate change will outweigh any increased uptake due to CO_2 fertilization or longer growing seasons; however, the uncertainty of this balance remains a significant obstacle in developing carbon budget models (Le Quéré *et al.*, 2009; IPCC, 2019).

Improving our ability to quantify the emissions of CO_2 and other GHGs from soils to the atmosphere is critical for accurate budgeting of the global C cycle and predicting future climate warming. To accurately predict soil CO_2 emissions, we need to have a mechanistic understanding of the processes in soil that contribute to CO_2 fluxes and their drivers. Decreasing uncertainty around global carbon emissions will be necessary moving forward if we are to reach our goals set out in the Paris Agreement of 2015 to limit the global increase in temperature to less than 2°C.

1.2 Organic matter decomposition processes

In the global C cycle, soil OM decomposition represents the mineralization of organic C that was previously fixed by living plant biomass and which eventually became deposited on or incorporated into the soil. The overall process of OM decomposition releases both C and other nutrients previously immobilized in biomass and provides energy to organoheterotrophic microorganisms through energy-yielding redox reactions. There are numerous and diverse processes involved in OM decomposition and the diversity of the soil microbial community has been shown to be linked to soil functionality and ecosystems services (Delgado-Baquerizo *et al.*, 2016). Therefore, improving our understanding of OM decomposition pathways in soil is a key first step in managing soil biogeochemical functioning.

Large, complex plant polymers (*e.g.*, cellulose) in the soil OM are too large for cells to take up and metabolize. Therefore, they must first be depolymerized, generally by extracellular hydrolytic or oxidase enzymes produced and excreted by soil microbes (Lynd *et al.*, 2002). Decomposition of most polymeric compounds in soil OM can be performed by hydrolytic enzymes that do not require oxygen (O_2), although the role of O_2 in controlling hydrolytic enzyme activity is still debated (Freeman *et al.*, 2001; Hall *et al.*, 2014). The result of hydrolysis of particulate organic carbon (POC) into smaller and smaller molecules is the release of dissolved organic carbon (DOC) to the soil water, and there is some evidence that this may be a rate-limiting step for the overall decomposition of soil carbon (Bengtson and Bengtsson, 2007).

1.2.1 Respiration

The term "soil respiration" is often associated with soil OM decomposition and soil CO_2 fluxes (there were over 500 articles published in the last 5 years with "soil respiration" in the title,

Web of Science). There is no clear definition for "soil respiration," but it is often used to describe CO_2 emitted from the soil surface. Likely, the CO_2-emitting process most commonly being referred to in many of these publications is microbial aerobic respiration, which is the oxidation of organic carbon using O_2 as a terminal electron acceptor (EA), and can be represented using the general chemical reaction:

$$"CH_2O" + O_2 \rightarrow CO_2 + H_2O, \quad (1.1)$$

where *"CH_2O"* is a generalized formula for organic carbon. Stable isotope analysis in a forest soil suggested that soil CO_2 production was sourced from DOC rather than POC, which is consistent with extracellular hydrolysis being required as a first step to make DOC accessible to be respired (Bengtson and Bengtsson, 2007). The amount of energy released by this reaction depends on the exact form of organic carbon being oxidized (LaRowe and Van Cappellen, 2011). However, using O_2 as the terminal EA will generally result in greater energy released than using an alternative EA (*e.g.,* sulfate); therefore, O_2 is thermodynamically the most favourable EA and the first to be used by organoheterotrophs.

Cellular respiration refers to a series of metabolic pathways in the cell which begins with glycolysis and eventually results in the oxidation of OM, production of adenosine triphosphate (ATP) and inorganic carbon, and the reduction of a terminal EA following reactions via an electron transport chain (Alberts *et al.,* 2008). When O_2 is not locally available, other EAs found in the environment can be used as the terminal EA in electron transport chains. A well-established cascading order of the favourability of paired reactions using various EAs exists, known as the thermodynamic redox ladder (Froelich *et al.,* 1979). For the oxidation of a given organic compound, EAs lower on the ladder are less thermodynamically favourable to serve as the oxidant and their reduction is generally inhibited by the availability of EAs higher on the ladder (LaRowe

and Van Cappellen, 2011). In one form of anaerobic respiration, denitrifiers oxidize organic carbon and reduce nitrogen in nitrate (NO_3^-), producing nitrogen gas, as well as nitrous oxide (N_2O) as an intermediate, which is a potent greenhouse gas (Richardson *et al.*, 2009). Other EAs that can be reduced in anaerobic respiration pathways include manganese, iron, sulfate, and CO_2 (though the exact metabolic pathways will differ). Therefore, if EAs are present and available in the soil environment, respiration pathways using some form of an electron transport chain may be used by the soil community (Figure 1-2).

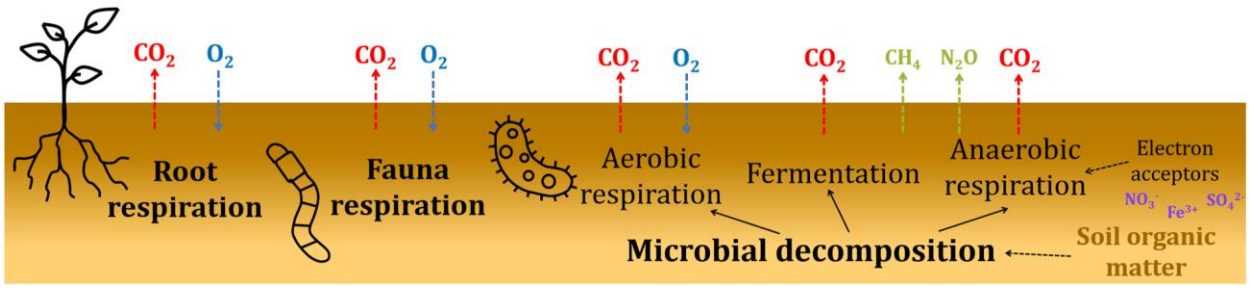

Figure 1-2: Variety of soil processes and metabolisms that may be described by the term "soil respiration" and involve the decomposition of organic matter. Aerobic respiration consumes O_2 and produces inorganic carbon (*i.e.*, CO_2). Anaerobic processes can include anaerobic respiration, which consumes other EAs and produces CO_2 (and some other gases, such as N_2O), fermentation, or methanogenesis, which produces CH_4 in addition to CO_2. Note that plants act as conduits for gas exchange between soil and the atmosphere (not shown).

1.2.2 Fermentation and methanogenesis

Fermentation is another metabolic pathway used in the decomposition of soil OM. In general, a reaction in which an organic compound is transformed into one or multiple other organic compounds, and which does not involve the reduction of an inorganic electron acceptor, is referred to as fermentation (LaRowe and Amend, 2019). In fermentation, organisms may proceed with ATP production via glycolysis only (*i.e.*, without an electron transport chain). In this case, NAD^+, a molecule that accepts electrons during glycolysis, is reduced to NADH and needs to be regenerated in order to continue acting as an EA in glycolysis (Alberts *et al.*, 2008). This requires

NADH to be oxidized to NAD^+ by reducing an organic compound – this is a form of fermentation. In natural settings, there are countless reactants that can be fermented and a great number of compounds that are products of fermentation, and therefore, fermenters carry out a diverse collection of reactions which makes fermentation a challenging process to characterize (LaRowe and Amend, 2019).

Fermentation is a multi-step process involving the primary fermentation of monomers (*e.g.*, glucose) to primary products (*e.g.*, alcohols, fatty acids), which then undergo secondary fermentation to low molecular weight organic acids (*e.g.*, acetate) (Megonigal *et al.*, 2004). Although fermentation itself yields little energy compared to respiration, it is a key step in anaerobic mineralization of organic carbon since many non-fermentative organisms rely on the products of fermentation as substrates for anaerobic respiration (Megonigal *et al.*, 2004). The fact that the hydrolysis of polymers and fermentation of monomers precede respiration pathways in the decomposition of OM is consistent with the findings that the supply of labile substrates controls the overall rates of OM decomposition (Bengtson and Bengtsson, 2007). Conversely, the presence of EAs then controls the relative contribution of different metabolisms (Schlesinger and Bernhardt, 2013).

If sufficient OM is present in the system, EAs could become entirely exhausted through respiration processes such as denitrification, iron and manganese reduction, sulfate reduction, and even the reduction of humic substances that can act as EAs (Lovley *et al.*, 1996). Methanogenesis can occur when the electron accepting capacity of the system is entirely depleted (Gao *et al.*, 2019). In hydrogenotrophic methanogenesis, CO_2 is reduced and H_2 is oxidized, producing methane (CH_4). In acetoclastic methanogenesis (also called acetate fermentation), acetate undergoes the following disproportionation reaction:

$$CH_3COOH \rightarrow CO_2 + CH_4. \quad (1.2)$$

Despite the 1:1 ratio of CO_2 and CH_4 produced during fermentative methanogenesis, the net rates of CH_4 production in soil are generally lower than those of CO_2 due to some degree of suppression of methanogenesis by the presence of EAs (both inorganic and organic), and the continuing production of CO_2 in respiration reactions (Knorr *et al.*, 2009). Even in EA-limited environments where methanogenesis is permitted, effluxes of CH_4 may be limited due to its consumption in CH_4 oxidation in oxic upper layers of the soil or rhizosphere (Segers, 1998). However, CH_4 emissions from low O_2 environments, such as water-logged soils, are still a major concern since CH_4 has a higher capacity than CO_2 to contribute to global warming (approximately 25 times more global warming potential than CO_2 over 100 years; Forster *et al.*, 2007).

1.3 Factors influencing organic matter decomposition in soil

1.3.1 Environmental factors

Soil moisture is a key factor controlling soil OM mineralization and resulting fluxes of GHGs. Aerobic soil respiration has been known to be maximal at mid-range soil moisture contents (Linn and Doran, 1984). At low moisture contents, microbial activity is limited by the diffusion of substrates and may also be affected by limited cell mobility (Schjønning *et al*., 2003; Or *et al*., 2007; Manzoni *et al*., 2011). Microbial processes at low soil moisture are also influenced by the cell stress response: cells must expend energy producing osmolytes to balance their water potential with that of their environment to avoid dehydration (Schimel *et al*., 2007). Microbial communities and species interactions can be affected by low moisture due to less pore connectivity and greater isolation at low moisture contents (Treves *et al*., 2003). Conversely, aerobic soil respiration is limited at high soil moisture contents by the diffusion of O_2 (Skopp *et al*., 1990). The balance of

the opposing influences of moisture and O_2 limitations result in the optimization of aerobic respiration at moderate soil moisture content (Figure 1-3).

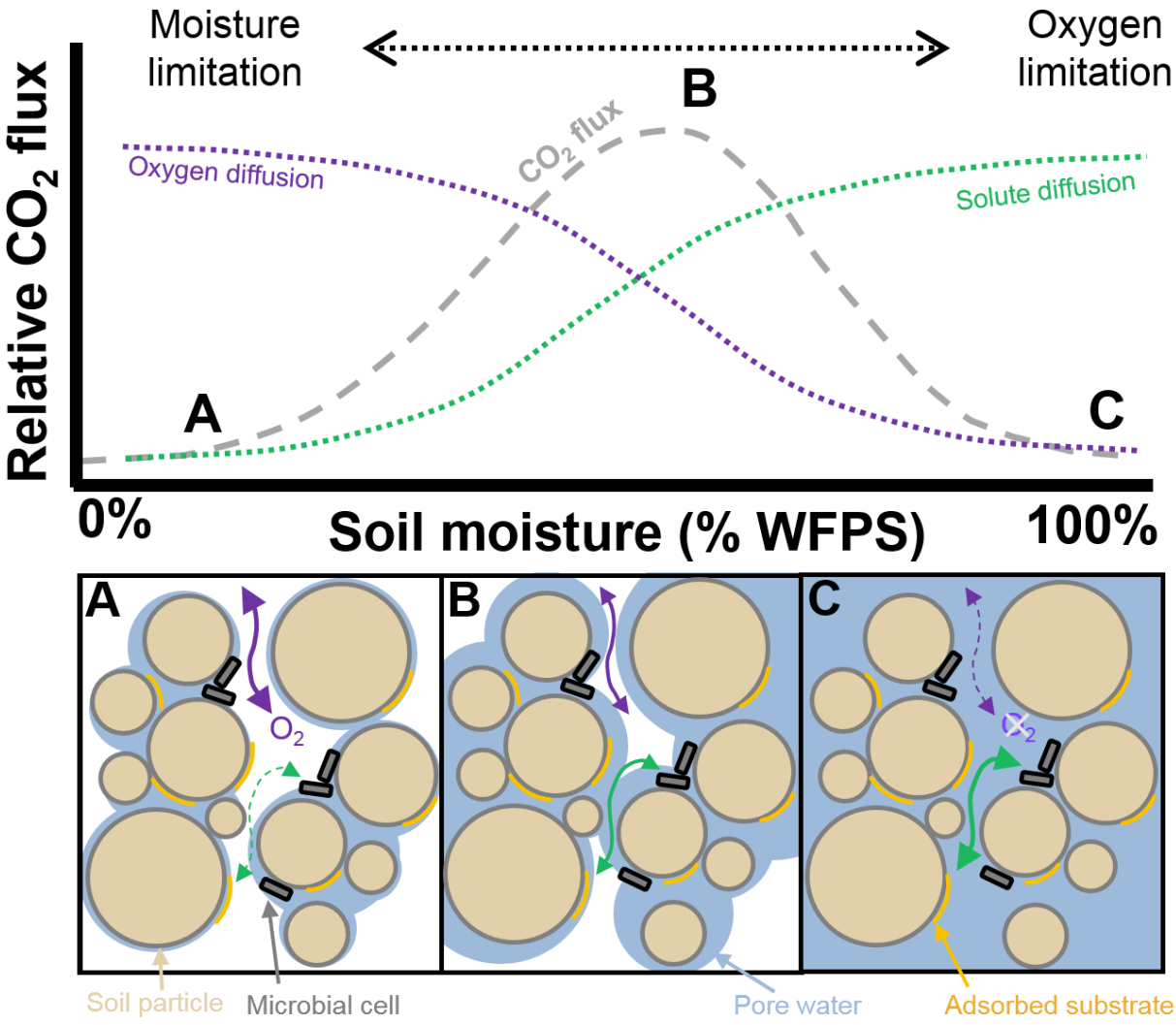

Figure 1-3: Classical representation of the effect of soil moisture on soil CO_2 fluxes. Top panel shows the relative diffusion of soluble substrates (green) and of O_2 (purple) and the resulting relative CO_2 fluxes according to the level of soil moisture. In a bottom panel, a schematic diagram shows the conditions under different levels of saturation (A, low soil moisture; B, moderate soil moisture; C, high soil moisture). Figure redrawn and modified from Moyano *et al.* (2013).

Since soil moisture and O_2 are closely linked, few studies have attempted to investigate these two factors separately, and the extent to which specific mechanisms influence CO_2 fluxes remains unclear. The relationship between moisture content, O_2 and CO_2 fluxes described above has long

been assumed but rarely validated experimentally. A recent study by Sierra *et al*. (2017) separated these factors' effects using a factorial experiment. Their results suggested that O_2 limitation is the main driver for low CO_2 fluxes at high soil moisture. Another study by McNicol and Silver (2014) demonstrated that both saturation and an anoxic headspace resulted in lower CO_2 fluxes from incubated soil samples than the control with moderate soil moisture and an oxic headspace. Their study also showed that under anoxic headspaces, saturation increased both anaerobic CO_2 production and CH_4 emissions compared to undersaturated soil, suggesting that soil moisture can influence C mineralization rates independently of O_2 availability.

Although the focus of many soil respiration studies has been aerobic respiration, investigating soil processes under anoxic conditions can be useful in achieving a greater understanding of O_2 and moisture effects on soil processes. A biodegradation study by Hack *et al.* (2015) confirmed that biodegradation rates of phenol and salicylic acid were higher under oxic than anoxic conditions. However, they additionally found that the relationship between decomposition rates and moisture content was different under oxic versus anoxic conditions. Oxic conditions resulted in the peak in fluxes at moderate moisture described above, but the anoxic conditions resulted in decomposition rates that increased with moisture and did not decrease at the highest moisture contents. This was possibly because the EA in this case (such as nitrate, for example, rather than O_2) was not limited by low gas diffusion at high soil moisture content. The mechanisms controlling soil processes under different levels of moisture still need more investigation under both oxic and anoxic incubation conditions.

Soil temperature is another major factor influencing soil microbial activity and CO_2 fluxes. Many soil biological processes have demonstrated strong temperature dependencies, with rates increasing with temperature up to an optimal level, and decreasing as temperature increases further

due to enzyme denaturation or thermodynamic limitations (Schipper *et al.*, 2014). In addition to influencing reaction rates directly, temperature can also affect rates indirectly, for example, by influencing the diffusion of substrates (Moyano *et al*., 2013). Temperature has been known to interact with other factors such as soil moisture and O_2 influencing CO_2 fluxes, and the temperature sensitivity of soil respiration can be variable across ecosystems and conditions (Davidson *et al*., 1998; Sierra *et al*., 2017). For example, multiple studies have observed that a soil moisture threshold exists below which temperature ceases to be the dominant factor controlling CO_2 fluxes (Lellei-Kovács *et al.*, 2011; Chang *et al.*, 2014). Therefore, soil CO_2 fluxes can depend on multiple factors and further research into their interactions is needed to identify which factors dominate under different environmental conditions.

1.3.2 Intrinsic factors

Factors inherent to the soil can also influence the rates of OM decomposition. In addition to the amount of OM available, one inherent property is the energetic, chemical and physical quality in terms of ease of decomposition and energy yielded by decomposition (*i.e.*, lability versus recalcitrance) of the soil OM substrate itself. The intrinsic quality of organic carbon substrates has previously been described by various indices, such as the carbon to nitrogen ratio (C:N), and some studies have conceptualized a thermodynamic basis for differences in substrate quality (Bosatta and Ågren, 1999; LaRowe and Van Cappellen, 2011). The importance of substrate quality was also demonstrated in a study by Jagadamma *et al.* (2014) which showed that the chemistry of added substrates not only affected the mineralization rates of the added substrate, but also of the native soil OM present. This so-called "priming" effect has also been observed when highly labile root exudate substrates enhance the bulk soil OM decomposition rates (Bengtson *et al.*, 2012). In

addition to the priming effect by labile substrates, nutrient enrichment can also enhance OM decomposition in soil (Hartley *et al.,* 2010).

Recently, the assumption that intrinsic chemical recalcitrance alone can explain OM stabilization in soil has changed to consider that some other physical or chemical mechanisms are involved in protecting OM from microbial decomposition (Lützow *et al.,* 2006). One physical soil property that may influence rates of C decomposition is soil texture. Clay content in soil has been hypothesized to influence the protection of OM from decomposition (Hassink, 1997). Small-sized particles in soil could protect OM from decomposition directly, through chemical associations with clay and silt particles, or indirectly, through physical protection inside aggregates, since texture can affect aggregate formation and stability (Six *et al.,* 2002). In their analysis, Six *et al.* (2002) summarized that OM stabilization in soil can be influenced by clay and silt content, clay type (2:1 vs. 1:1) and clay and silt size ranges. Previous studies have investigated the effect of clay mineralogy on the stabilization of OM in soil (Pronk *et al.,* 2013; Barré *et al.,* 2014). In studies that used and developed models to predict OM decomposition (*e.g.,* RothC, Century and CORPSE), clay content has been included as a parameter influencing the protection of soil OM from decomposition (Parton *et al.,* 1983; Coleman *et al.,* 1997; Sulman *et al.,* 2014). However, the protective effect of soil clay (or clay + silt) content can be difficult to model mechanistically since many different direct and indirect effects are involved (Plante *et al.,* 2006).

While many studies have looked at the stabilizing effect of clay content on soil OM, few studies have considered the combined influences of soil texture and soil moisture on OM decomposition. Several modelling efforts have included parameters for soil texture and have hypothesized an interactive effect between soil moisture and texture, namely that soil texture will influence the position of the peak or the shape of the curve for the relationship between CO_2 fluxes

and moisture (Moyano *et al.,* 2013; Ghezzehei *et al.,* 2019; Tang and Riley, 2019). However, very little direct experimental evidence exists to test the hypotheses put forward in these modelling studies. Currently, these models can be validated with large data syntheses using data collected from a wide range of soil types (*e.g.,* Moyano *et al.,* 2012), which, while useful in identifying patterns at this scale, are ill-equipped to test hypotheses about the mechanisms involved in these relationships. Tightly controlled experiments where soil texture and soil moisture can be manipulated are needed to isolate the effects of these factors.

1.4 Climate change impacts on soil processes

Climate change is significantly altering the hydrological cycle, which influences soil moisture conditions in many regions. Although global models disagree on whether precipitation totals will increase or decrease, there is agreement that precipitation events are becoming more extreme, including in southern Ontario (Deng *et al.*, 2016; Donat *et al*., 2016). Increases in extreme precipitation will mean that more of the total rainfall will occur as heavy precipitation during extreme events with longer intervening periods of dryness (Easterling, 2000). These changes to precipitation patterns and resulting changes in soil moisture regimes may affect microbial activity in soil (Poll *et al.,* 2013). A study by Harper *et al.* (2005) showed that seasonal mean CO_2 fluxes decreased with a decrease in total rainfall amounts, and with longer intervening dry periods between rainfall events. Therefore, whether climate change has an impact on precipitation amounts or on precipitation timing and intensity, soil CO_2 emissions will likely be affected. In addition to precipitation changes, thawing of permafrost could alter hydrologic conditions resulting in greater soil drainage and changes in soil moisture and O_2 conditions and thus, changes to CO_2 and CH_4 emissions (Lawrence *et al.,* 2015).

The potential impacts of climate change-induced changes to soil temperature regimes on soil OM decomposition and resulting GHG emissions remain uncertain. The future impacts of increased temperature on soil CO_2 emissions have been debated in the literature for years, with some arguing that rising temperatures will accelerate soil CO_2 emissions (Davidson *et al.,* 2000; Hartley *et al.,* 2008) and others suggesting that soil C is tolerant to changes in temperature (Giardina and Ryan, 2000). The sensitivity of soil organic C to rising temperatures is difficult to characterize and predict, but it would be highly concerning if there is a net positive feedback (Davidson and Janssens, 2006). A recent study has already shown that warming in northern regions has caused permafrost soils to emit more CO_2 in the winter than they take up in the growing season *(*Natali *et al.,* 2019). Reducing the uncertainty in our predictions of future soil CO_2 emissions will require more experimental, field, and model assessments of the sensitivity of soil OM stabilization and decomposition to environmental change.

1.5 Thesis objectives

The overall objective of this thesis was to advance the process-based understanding of how soil moisture affects organic C decomposition rates in soil by quantifying and considering the production (and emission) of CO_2 and CH_4. The specific objectives for Chapter 2 of this thesis were to:

1) Experimentally validate the previous assumption that the optimization of CO_2 fluxes at moderate soil moisture results from the minimization of the combined limitation effects of soil moisture and O_2,
2) Develop a model for predicting soil CO_2 fluxes as a function of soil moisture that explicitly accounts for the contribution of anaerobic sources to total CO_2 production.

The specific objectives for Chapter 3 of this thesis were to:

3) Summarize the current understanding of the effects of soil texture on soil OM decomposition and its interaction with soil moisture, including existing models that provide a framework to test hypotheses regarding these potential effects,
4) Develop an experimental method for examining the effects of both soil texture and soil moisture on CO_2 fluxes and present results from a factorial batch experiment.

1.6 Thesis outline

This thesis consists of four chapters. Chapter 1 includes the general introduction and literature review on soil OM as an important global C reservoir, the processes involved in OM decomposition and their drivers. Chapter 2 consists of a co-authored manuscript of which I am the first author and which will be modified and submitted to *Proceedings of the National Academy of Sciences of the United States of America* (*PNAS*; impact factor: 9.58). Thus, it was written as a stand-alone document but has been modified slightly to be consistent with formatting and numbering of sections, figures and equations. The chapter describes a factorial batch experiment examining the separate effects of soil moisture and O_2 on CO_2 fluxes. Chapter 3 consists of a short literature review about the role of soil texture in the relationship between soil moisture and CO_2 fluxes and it discusses the results of a factorial batch experiment. Chapter 4 consists of overall conclusions, recommendations and future research opportunities. Following Chapter 4 is the reference list and appendix. The appendix includes additional experimental results that were not included in Chapter 2. Since Chapter 2 does not describe the materials and methods used for some of these additional analyses, some additional text describing the methodology is included in the appendix.

Representing the relationship between soil CO_2 fluxes and soil moisture: Anaerobic sources explain fluxes at high moisture content

L. Fairbairn[1*], F. Rezanezhad[1,2], M. Gharasoo[1], C.T. Parsons[1,3], M.L. Macrae[4] and P. Van Cappellen[1,2]

[1] Ecohydrology Research Group, Department of Earth and Environmental Sciences, University of Waterloo, Waterloo, Ontario, Canada, N2L 3G1
[2] Water Institute, University of Waterloo, Waterloo, Ontario, Canada, N2L 3G1
[3] Environment and Climate Change Canada, Burlington, Ontario, Canada, L7S 1A1
[4] Department of Geography and Environmental Management, University of Waterloo, Waterloo, Ontario, Canada, N2L 3G1

[*]Corresponding author: Linden Fairbairn
Ecohydrology Research Group, Department of Earth and Environmental Sciences, University of Waterloo, 200 University Avenue West, Waterloo, Ontario, Canada N2L 3G1
Phone: (519) 888-4567, Ext. 31798
lgfairbairn@uwaterloo.ca

This chapter will be modified for submission to *Proceedings of the National Academy of Sciences of the United States of America (PNAS).*

2 Representing the relationship between soil CO_2 fluxes and soil moisture: Anaerobic sources explain fluxes at high moisture content

2.1 Introduction

The efflux of carbon dioxide (CO_2) from soils represents a massive component of the global carbon (C) cycle (Raich and Schlesinger, 1992), where annual effluxes have been estimated at 75 Pg C yr^{-1} (Schlesinger, 1977; Raich and Potter, 1995), much greater than emissions from anthropogenic sources such as fossil fuel use and cement production (9.5 Pg C yr^{-1} in 2010; Peters *et al.*, 2013). Losses of C from terrestrial ecosystems are largely balanced by uptake through primary production (previous studies have suggested a slight net sink; Schimel, 1995), but there is concern that, due to the magnitude of these annual fluxes, even relatively minor perturbations to this balance would have a major impact on atmospheric CO_2 levels. Soil CO_2 fluxes are affected by environmental factors such as soil temperature and moisture, and there is currently great interest in understanding the responses of soil CO_2 fluxes to changes in these factors due to current and future climates (Orchard and Cook, 1983; Lloyd and Taylor, 1994; Davidson and Janssens, 2006; Singh *et al.*, 2010).

Soil moisture has been recognized as a key factor controlling soil CO_2 fluxes, which are known to be maximal at moderate soil moisture contents (Figure 1-3; Linn and Doran, 1984; Moyano *et al.*, 2012). At low soil moisture, CO_2 fluxes are limited by the diffusion of organic carbon substrates and by physiological stress to the cells (Schjønning *et al.*, 2003; Or *et al.*, 2007; Manzoni *et al.*, 2011) and at high soil moisture, aerobic respiration is limited by the diffusive flux of O_2 (Skopp *et al.*, 1990). These opposing influences of moisture and O_2 result in the peak in CO_2 fluxes at moderate soil moisture. Though soil moisture and O_2 are known to be linked and both influence soil microbial activity, few efforts have been made to examine the effects of these two

factors separately (McNicol and Silver, 2014; Sierra *et al.*, 2017), and the extent to which specific mechanisms influence CO_2 fluxes remains unclear.

Many existing models consider the influence of soil moisture on rates of CO_2 fluxes. Some soil moisture functions describe the balance between organic C substrate and O_2 diffusion limitations using dual Michaelis-Menten kinetics (Davidson *et al.*, 2012; Moyano *et al.*, 2013) or some other co-limited relationship (Yan *et al.*, 2018). The development of these models has been focused towards a conceptual understanding of the coupled effects of soil moisture and O_2 on aerobic soil respiration. However, most do not consider the contributions of anaerobic processes to CO_2 fluxes. Soil anaerobiosis is a common feature of wetland soils, but O_2 depletion can also persist in upland soils (Silver *et al.*, 1999; Brewer *et al.*, 2018). Soil O_2 can vary both spatially, such as within soil aggregates (Sexstone *et al.*, 1985; Pallud *et al.*, 2010) and particulate organic matter (Parkin, 1987), and temporally, such as following intense precipitation (Schuur and Matson, 2001). A discrepancy exists currently between models that predict zero CO_2 fluxes under saturated conditions due to the absence of O_2 (Figure 1-3) and data sets that show non-zero fluxes at saturation (*e.g.*, Moyano *et al.*, 2012). Therefore, by ignoring anaerobic sources of CO_2, existing soil CO_2 flux models lack a comprehensive understanding of the controls of anaerobic processes on soil C decomposition.

In this study, our objective was to perform a series of soil incubation experiments where the CO_2 fluxes were measured from soil samples of different moisture contents under both oxic and anoxic headspace incubations. The factorial nature of this experimental design allowed us to decouple the effects of these two factors which was useful to better understand the mechanisms involved, and to validate a long-standing assumption about the effects of soil moisture on soil CO_2 fluxes. Our hypothesis was that CO_2 fluxes would follow the above described trend (the peak in

CO_2 fluxes at moderate soil moisture) in the oxic conditions; but, in the anoxic conditions, fluxes would be maximal at the highest soil moisture since O_2 was absent and thus its availability would not be influenced by increasing soil moisture. In addition to monitoring CO_2 fluxes, we also measured methane (CH_4) fluxes and characterized the soil pore water chemistry to get a better understanding of the microbial processes occurring. The results highlight the contribution of anaerobic processes to soil CO_2 fluxes and how considering these sources helps explain the observed relationship of soil CO_2 fluxes with soil moisture.

2.2 Materials and methods

2.2.1 Soil collection and preparation

An agricultural soil was chosen for the incubation experiments. The CO_2 fluxes from agricultural soils have received relatively little attention, despite agricultural lands occupying approximately 40% of global land area (Foley *et al.*, 2005), the potential for increased C sequestration through management practices (Paustian *et al.*, 2000), and the implications of soil organic matter (OM) turnover for soil health (Doran, 2002). Soil was collected from an agricultural field at the ***rare*** Charitable Research Reserve (www.raresites.org) located in Cambridge, Ontario, Canada (Figure 2-1; 43°22'39.80"N, 80°22'07.28"W). The field was planted in soy for the preceding season and had not yet been harvested at the time of soil sampling in late summer. In previous years, the field has been rotated in soy, corn, and wheat and red clover.

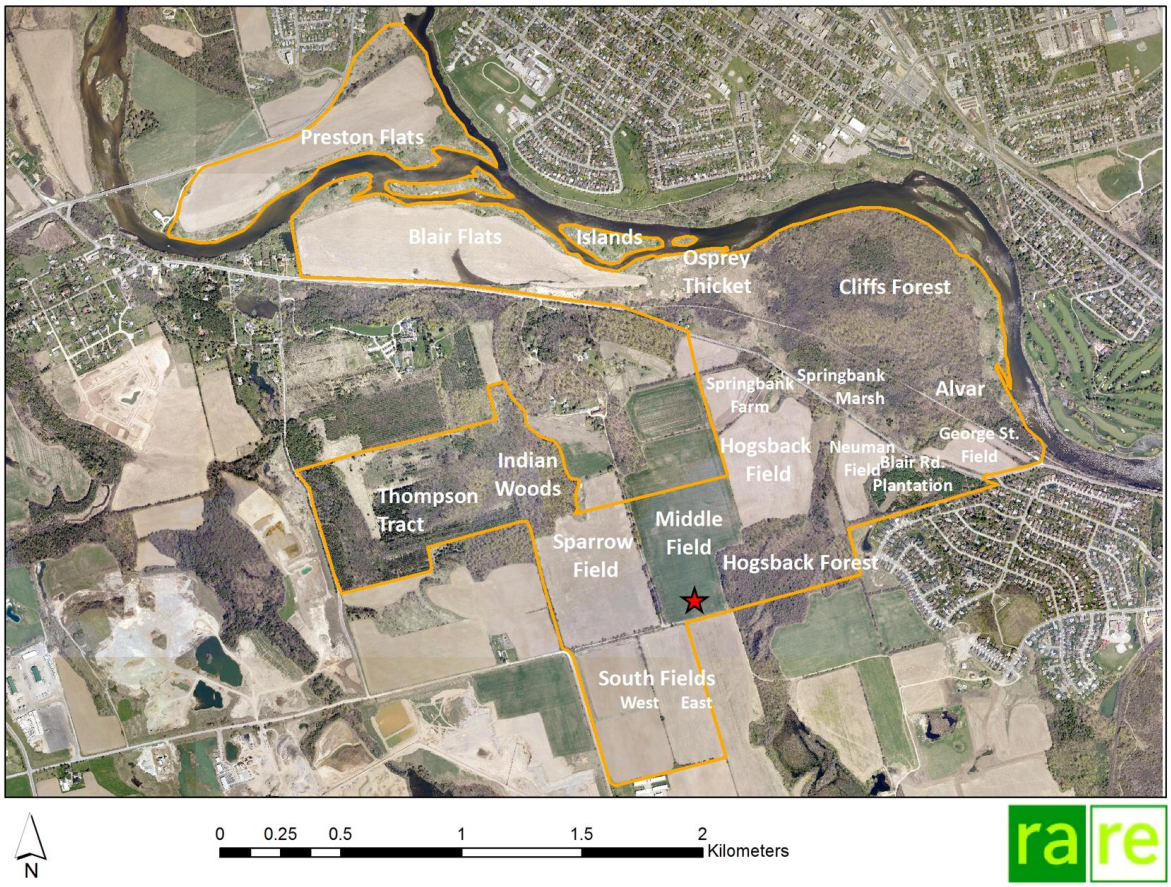

Figure 2-1: Map of ***rare*** Charitable Research Reserve in Cambridge, Ontario. Soil was collected from the Middle Field and the location of sampling is marked by a star. In 2018, this field was planted in soy. Map courtesy of ***rare***.

Soil was sampled to a depth of approximately 15 cm and then sieved to 4 mm and air dried. Homogenized soil samples were used to determine moisture content (θ), porosity (ϕ), bulk density (ρ_b), particle size distribution and solid-phase chemical compositions using standard procedures. Measurements of θ , ϕ , and ρ_b were determined gravimetrically following the method of Gardner (1986), based on the sample volume, the sample saturated mass and the oven-dried (24 h at 105°C) mass and ϕ was calculated assuming a particle density of 2.65 g/cm^3. Values of ρ_b and ϕ were 1.22 g cm^{-3} and 0.54, respectively. Particle size distribution was analyzed using the pipette method (Gee and Bauder, 1986). Sand, silt and clay fractions were 49%, 39% and 12%, respectively. Total organic and inorganic carbon and total nitrogen in the soil sample were measured on a CHNS

Carbo Erba analyzer (method detection limit, MDL: 0.1 mg g^{-1}) and were determined as 17.2, 1.3 and 1.6 mg g^{-1}, respectively.

Allocations of 300 g of homogenized and air-dried soil were prepared in 500 mL glass jars and the soil surface area was approximately 35 cm^2. Moisture content was adjusted with water prepared to closely match the pH, electrical conductivity and ionic composition of groundwater from the field site containing $NaHCO_3$ (0.37 mM), KCl (0.02 mM), $CaCl_2$ (1.75 mM), $MgCl_2$ (1.15 mM), and $CaSO_4$ (0.2 mM) in ultrapure deionized water. This artificial water was used to minimize disturbances to the native microbial community upon large changes in soil moisture due to osmotic or pH shock (Killham, 1985; Halverson *et al.*, 2000). The soil moisture levels were achieved by adding 0, 20, 40, 60 or 80 mL of the artificial water to soil and homogenizing the sample, corresponding to moisture levels of approximately 30%, 45%, 65%, 80% and 100% water-filled pore space (WFPS), respectively (Figure 2-2). Moisture content as the percentage WFPS was calculated using the calculated soil porosity and the amount of water added plus residual water present in the air-dried soil.

2.2.2 Incubation experiment

The treatments included five moisture contents, two oxygen conditions, and all were prepared in triplicate (5 × 2 × 3 = 30 samples in total). One additional sample of each of the five moisture contents was prepared and sacrificed for initial pore water analyses at the beginning of the experiment. Incubations began once the soil moisture had been adjusted; half of the thirty soil samples were incubated in an anaerobic chamber (nitrogen gas with <0.1% O_2 and between 1 and 2.5% hydrogen) at 25 ± 2°C and half in an incubator (Innova® 42 Incubator Shaker, New Brunswick Scientific™) set at 25°C. Soil samples in the incubator thus had oxic headspaces (hereafter referred to as oxic samples, though O_2 status of these soil samples depended on the

moisture content), while soil samples incubated in the anaerobic chamber had anoxic headspaces (hereafter referred to as anoxic samples).

Except during the gas flux measurements, the jars were left open during the entirety of the incubation period. Since humidity control was not available, samples in the incubator had to be contained in a partially opened plastic bag containing a soaked sponge to minimize evaporation while still allowing adequate air exchange. Regardless, the moisture contents of all soil samples were maintained by monitoring the weight and replacing any water lost to evaporation by misting the soil each day with MilliQ water equilibrated with either the atmosphere or with the nitrogen atmosphere of the anaerobic chamber (daily evaporative losses were typically between 1 and 3 mL). Soil samples were incubated in these conditions for a period of 21 days.

For all 30 soil samples, flux measurements of CO_2, CH_4 and N_2O and headspace O_2 concentrations were measured following the 21-day incubation. Prior to the end of the incubation, gas fluxes were measured intermittently to confirm that the CO_2 fluxes has reached relatively stable rates. Following the gas flux measurements, all soil samples were sub-sampled for pore water chemistry analyses (see section *2.2.3*). Pore water was extracted and analyzed for dissolved organic carbon (DOC), dissolved inorganic carbon (DIC), major anions, organic acids, pH and electrical conductivity (EC). Subsamples of soil were also extracted with 0.5 M potassium sulfate (K_2SO_4) and analyzed for DOC and DIC. Analyses were performed on both the final soil samples following the incubation and on the additionally prepared initial soil samples.

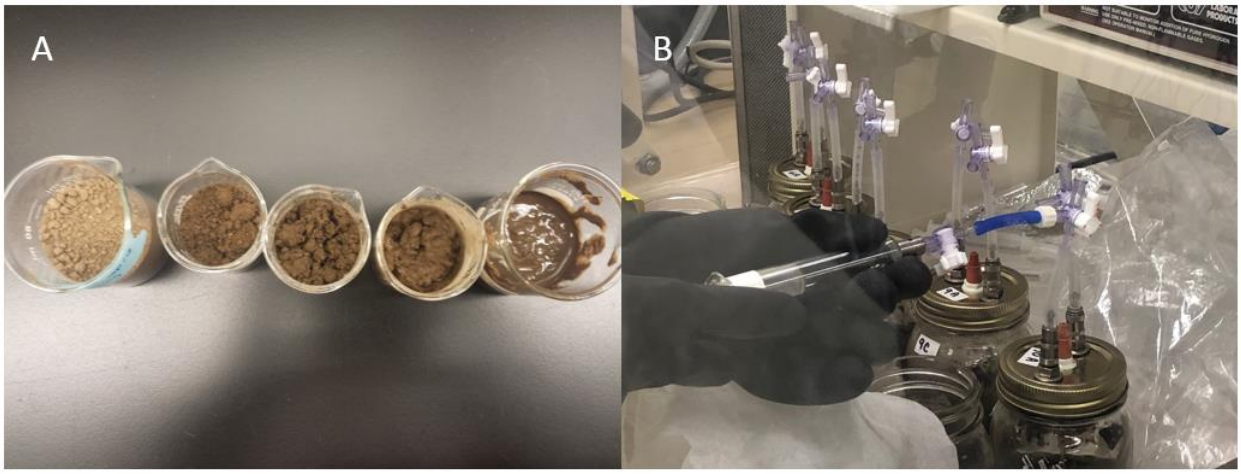

Figure 2-2: Photos of (A) five different soil moisture levels (increasing from left to right) and of (B) headspace gas sampling of sample jars in an anaerobic chamber.

2.2.3 Analytical methods

Gas flux measurements

Gas fluxes in the headspace of the jars were measured by closing the headspaces for 30 minutes using lids fitted with ports for gas sampling. The headspace gases were sampled before and after the closed incubation and the gas samples were analyzed for concentrations of CO_2, CH_4, N_2O and O_2. Gas concentrations were measured using a Shimadzu Gas Chromatograph (Model GC-2014) equipped with a flame ionization detector and methanizer (for CO_2 and CH_4), electron capture detector (for N_2O) and thermal conductivity detector (for O_2). The gas fluxes (F_{gas}, nmol cm^{-3} soil hr^{-1}) were obtained from the rate at which the headspace gas concentration increased after closure and were calculated by:

$$F_{gas} = \frac{\Delta C_{gas} V}{RT\Delta t V_{soil}}, \tag{2.1}$$

where ΔC_{gas} is the change in gas concentration over the closed incubation period (μmol mol^{-1}), V is the volume of the headspace (L), R is the gas constant (0.082057 L atm K^{-1} mol^{-1}), T is the temperature (˚K), Δt is the time of the closed incubation (hr), and V_{soil} is the volume of the soil

sample (cm^3; soil dry mass × bulk density). O_2 concentrations as percent were measured to confirm anoxic headspaces in the anoxic samples.

Pore water geochemistry

For pore water geochemical analyses, a portion of each soil sample was centrifuged at 5000 rpm for 30 minutes and the supernatant pore water filtered through a 0.45 µm membrane filter (polypropylene syringe filters, VWR). Pore water could only be extracted for soil samples of 65%, 80% and 100% moisture contents, since the lower moisture contents (30% and 45%) were too dry. Filtered pore water was analyzed for pH and EC using handheld meters (LAQUA Twin meters, model Horiba B-213). Pore water concentrations of DOC (MDL 6 µmol/L) in filtered pore water samples that had been acidified to pH <3 using 1M HCl were measured using a total organic carbon analyzer (Shimadzu TOC-LCPH/CPN). Non-acidified samples were also analyzed for DIC (MDL 3 µmol/L) using the same analyzer. Approximately 1 mL of pore water was filtered through a 0.2 µm membrane filter (Thermo Scientific Polysulfone filter) and frozen for later analysis of major anions including chloride (Cl^-), nitrate (NO_3^-) and sulfate (SO_4^{2-}) using ion chromatography (IC, Dionex ICS-5000 with a capillary IonPac® AS18 column; MDL 0.076, 0.050, and 0.127 mg/L, respectively). These pore water samples were also analyzed using an analytical column for the following low molecular weight organic acids: acetate (MDL in mg/L: 0.057), lactate (0.036), propionate (0.060), formate (0.066), butyrate (0.059), pyruvate (0.062), succinate (0.063) and citrate (0.343).

In addition to the direct pore water extraction by centrifugation, soil samples of all soil moisture contents were also characterized using the K_2SO_4 extraction method (Wang *et al.*, 2003; Makarov *et al.*, 2013). In this method, 5 g bulk soil were extracted in 25 mL 0.5 M K_2SO_4 in a tube rotator for 30 minutes, then centrifuged at 3500 rpm for 15 minutes, filtered through a 0.45

μm membrane filter (polypropylene syringe filters, VWR) and analyzed for DOC and DIC using the analytical methods described above.

2.2.4 Model description and calibration

The CO_2 flux data in both oxic and anoxic incubations was simulated using a model that describes the total CO_2 flux from soil (R_{CO2}) as the sum of aerobic respiration (R_{Ox}) and anaerobic (R_{An}) production of CO_2:

$$R_{CO_2} = R_{Ox} + R_{An}. \tag{2.2}$$

Aerobic respiration of dissolved organic carbon is represented using mixed dual Michaelis-Menten kinetics and depends on both the availability of the DOC and O_2, similarly to the DAMM model (Davidson *et al.*, 2012). The rate, in the units of nmol cm^{-3} soil hr^{-1}, is:

$$R_{Ox} = V_{max,Ox} \frac{DOC_{av}}{k_{c,Ox} + DOC_{av}} \frac{O_{2,liq}}{k_o + O_{2,liq}}, \tag{2.3}$$

where $V_{max,Ox}$ is the maximum conversion rate of aerobic respiration, DOC_{av} and $O_{2,liq}$ are the concentrations of DOC substrate and O_2 available at the reaction site, and $K_{c,Ox}$ and K_o are the half-saturation constants for DOC and O_2 for aerobic respiration, respectively.

Available DOC (DOC_{av}, μmol cm^{-3} soil) and O_2 ($O_{2,liq}$) are estimated using relationships from the DAMM model which are functions of the water and air-filled pore space, respectively:

$$DOC_{av} = D_l[DOC]\theta^n, \tag{2.4}$$

$$O_{2,liq} = 0.209 D_g(\phi - \theta)^{4/3}, \tag{2.5}$$

where *[DOC]* represents the DOC concentration in the soil water, D_l and D_g are dimensionless diffusion coefficients for aqueous and gas, respectively, n is an empirical parameter relating the

amount of available DOC to the amount dissolved, and 0.209 is the volumetric fraction of O_2 in air (L L^{-1}). Volumetric water content, θ, is calculated as:

$$\theta = \theta_s \phi + \theta_r (1 - \theta_s), \tag{2.6}$$

where θ_s is the water saturation (WFPS) and θ_r is the residual water content, the value of which was assumed insignificant in this study. Air-filled porosity is represented as porosity minus the volumetric water content ($\phi - \theta$).

In addition to aerobic respiration, this model also considers anaerobic sources of CO_2 and lumps all anaerobic processes into one term (R_{An}):

$$R_{An} = V_{max,An} \frac{DOC_{av}}{k_{c,An} + DOC_{av}} \frac{k_{in}}{k_{in} + O_{2,liq}}, \tag{2.7}$$

where $V_{max,An}$ is the maximum conversion rate, $k_{c,An}$ is the half-saturation constant for this reaction and k_{in} is an inhibition coefficient for the inhibitory effect of O_2 on anaerobic reactions. Which anaerobic processes are theoretically included in this term and the decision to lump all anaerobic processes into one term is further discussed in sections *2.4.2* and *2.4.3*.

In the oxic incubations, CO_2 fluxes can result from both aerobic and anaerobic production, and the contribution of each depends on the moisture content. Substituting Eqs. (2.3) – (2.5) and Eq. (2.7) into Eq. (2.2) gives the following equation for CO_2 fluxes in the oxic incubation:

$$\begin{aligned}(R_{CO_2})_{Ox} = {} & V_{max,Ox} \frac{D_l [DOC]_{Ox} \theta^{n_{Ox}}}{k_{c,Ox} + D_l [DOC]_{Ox} \theta^{n_{Ox}}} \frac{0.209 D_g (\phi - \theta)^{4/3}}{k_o + 0.209 D_g (\phi - \theta)^{4/3}} \\ & + V_{max,An} \frac{D_l [DOC]_{Ox} \theta^{n_{Ox}}}{k_{c,An} + D_l [DOC]_{Ox} \theta^{n_{Ox}}} \frac{k_{in}}{k_{in} + 0.209 D_g (\phi - \theta)^{4/3}}.\end{aligned} \tag{2.8}$$

In the anoxic incubations, however, only anaerobic production of CO_2 can occur. Therefore, the model used to fit the anoxic CO_2 flux data can be further simplified:

$$(R_{CO_2})_{An} = V_{max,An} \frac{D_l [DOC]_{An} \theta^{n_{An}}}{k_{c,An} + D_l [DOC]_{An} \theta^{n_{An}}}, \quad (2.9)$$

since in the absence of O_2, R_{Ox} equals zero and the inhibition term in R_{An} approaches 1.

Values for unknown parameters $V_{max,Ox}$, $V_{max,An}$, k_o, $k_{c,An}$, n_{Ox} and n_{An} for our system were estimated by simultaneously fitting the oxic CO_2 flux data to Eq. (2.8) and the anoxic CO_2 flux data to Eq. (2.9). The fitting procedure was done by ReKinSim (Gharasoo *et al.*, 2017) and the 95% error bounds were calculated from the covariance matrix in the manner analogous to previous applications of ReKinSim (Ehrl *et al.*, 2018; Marozava *et al.*, 2019).

Due to the logistic limitations on the number of gas flux measurements that could be performed in this experiment, the number of CO_2 flux data points is limited to ten (5 moisture contents, 2 O_2 conditions). To avoid problems with parameter equifinality, measured or literature values were assumed for all other parameters wherever possible (Table 2.1). Additionally, we used a piecewise cubic-hermite interpolating technique (Fritsch and Carlson, 1980) to increase the number of data points. This improved the quality of the fitting and greatly reduced the estimated parameters' uncertainty ranges.

Table 2.1: Parameter values derived from measurements, calculations or literature values

Parameter	*Value*
Porosity (ϕ)	0.54[m]
Residual water content (θ_r)	0
Dissolved organic carbon in oxic incubation ($[DOC]_{Ox}$)	1.99 µmol cm^{-3} soil[m]
Dissolved organic carbon in anoxic incubation ($[DOC]_{An}$)	28.26 µmol cm^{-3} soil[m]
Dimensionless diffusion coefficient of solute (D_l)	3.17[1]
Dimensionless diffusion coefficient of oxygen (D_g)	1.67[1]
Half saturation constant for DOC for aerobic ($k_{c,Ox}$)	0.0829 µmol cm^{-3} soil[1]
Oxygen inhibition coefficient for anaerobic reaction (k_{in})	0.02 µmol cm^{-3} soil[2]

[1]Davidson *et al.* 2012; [2]Van Cappellen & Wang 1995; [m]Experimentally measured or calculated value

2.3 Results

2.3.1 Gas fluxes

The average O_2 concentration during gas flux measurements was 21.0% ± 0.1% SD for the oxic incubations and 0.1% ± 0.01% SD (MDL 0.05%) for the anoxic incubations, confirming the virtual absence of O_2 in the headspaces of the anoxically incubated samples. Though the magnitude of CO_2 fluxes varied slightly with minor temperature fluctuations over time, overall relationships between soil moisture and CO_2 fluxes (*e.g.*, at which moisture content peak fluxes occurred) observed at the end of the experiment for both the oxic and anoxic incubations were unchanged from those observed earlier in the incubations. Therefore, only the final CO_2 flux measurements have been reported (mean ± standard deviation, n=3). CH_4 fluxes were more dynamic and therefore some earlier methane measurements have been reported which are needed to understand the development of methanogenic conditions. CO_2 fluxes (Figure 2-3) were maximal in the 65% WFPS samples under oxic conditions (31.2 ± 1.5 nmol cm^{-3} soil hr^{-1}) and decreased with moisture content towards both the low (30% WFPS) and high (100%) moisture contents. Under anoxic conditions, CO_2 fluxes increased with moisture content up to a maximum at 100% WFPS (21.8 ± 2.2 nmol cm^{-3} soil hr^{-1}), which was similar in magnitude to the 100% WFPS samples under oxic headspace conditions.

The fluxes of CH_4 were not measurable or were close to zero (0.06-0.17 nmol cm^{-3} soil hr^{-1}) in the oxic samples (Figure 2-4). In the anoxic samples, CH_4 fluxes were close to zero (0.04-0.12 nmol cm^{-3} soil hr^{-1}) at 30% and 45% WFPS, but started to increase slightly around 65% WFPS samples and then drastically increased to a maximum (21.0 ± 0.8 nmol cm^{-3} soil hr^{-1}) at 100% WFPS, very close to the molar flux of CO_2 from the same soil samples. Unlike the CO_2 fluxes, CH_4 fluxes were dynamic over time. About 1 week before the final measurements, measured CH_4

fluxes in the anoxic incubations were much lower, reaching a maximum of 1.0 nmol cm^{-3} soil hr^{-1} at 100% WFPS, and <0.6 nmol cm^{-3} soil hr^{-1} about 2 weeks before. Nitrous oxide (N_2O) concentrations were not detected in the headspaces of the anoxic samples, and although small concentrations were measured in the oxic samples (~0.5 ppm), no fluxes were measurable.

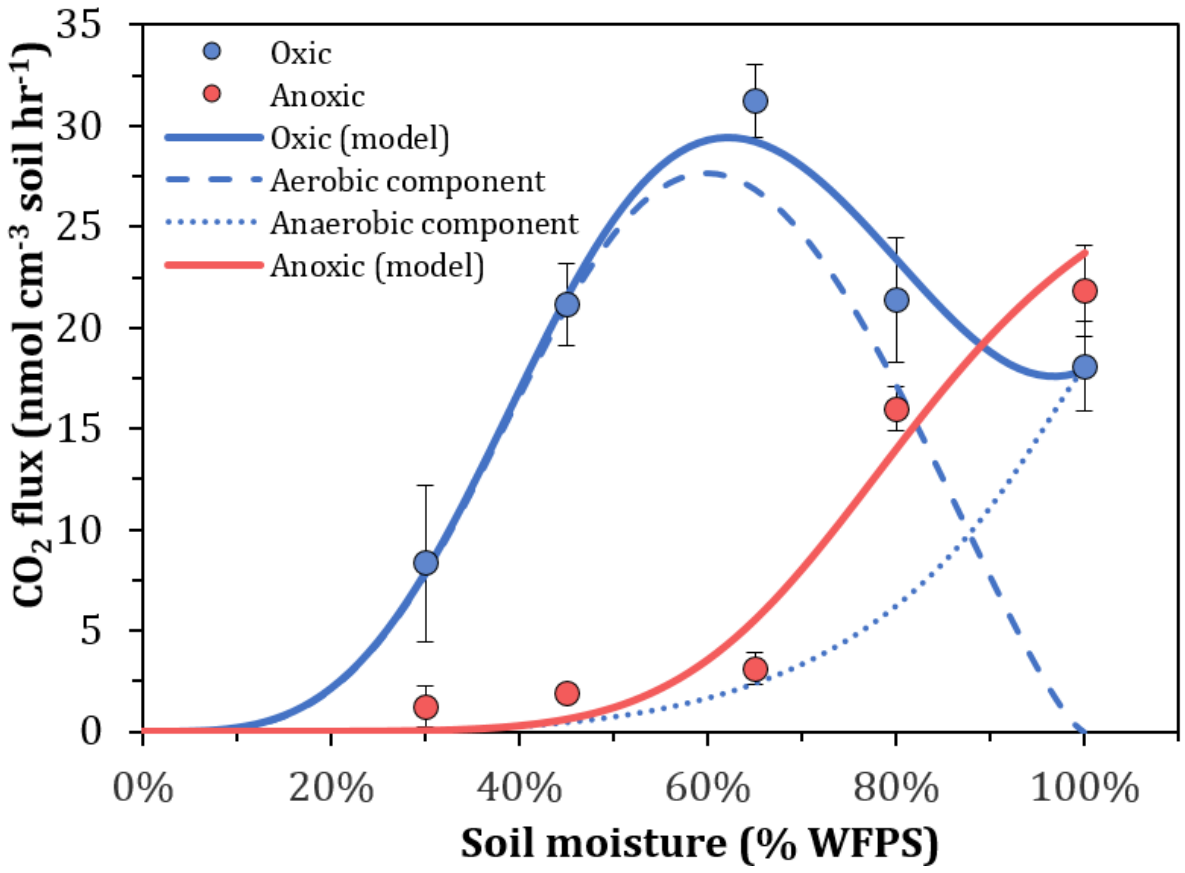

Figure 2-3: Measured CO_2 effluxes at the end of the incubations for oxic (blue circles) and anoxic (red circles) soil samples at different moisture contents with standard deviation (n=3). Oxic data fit with model combining aerobic and anaerobic processes (solid blue line) and anoxic data fit with model including only anaerobic processes (solid red line). Aerobic (dashed blue line) and anaerobic (dotted blue line) components of the total oxic CO_2 flux model are also shown.

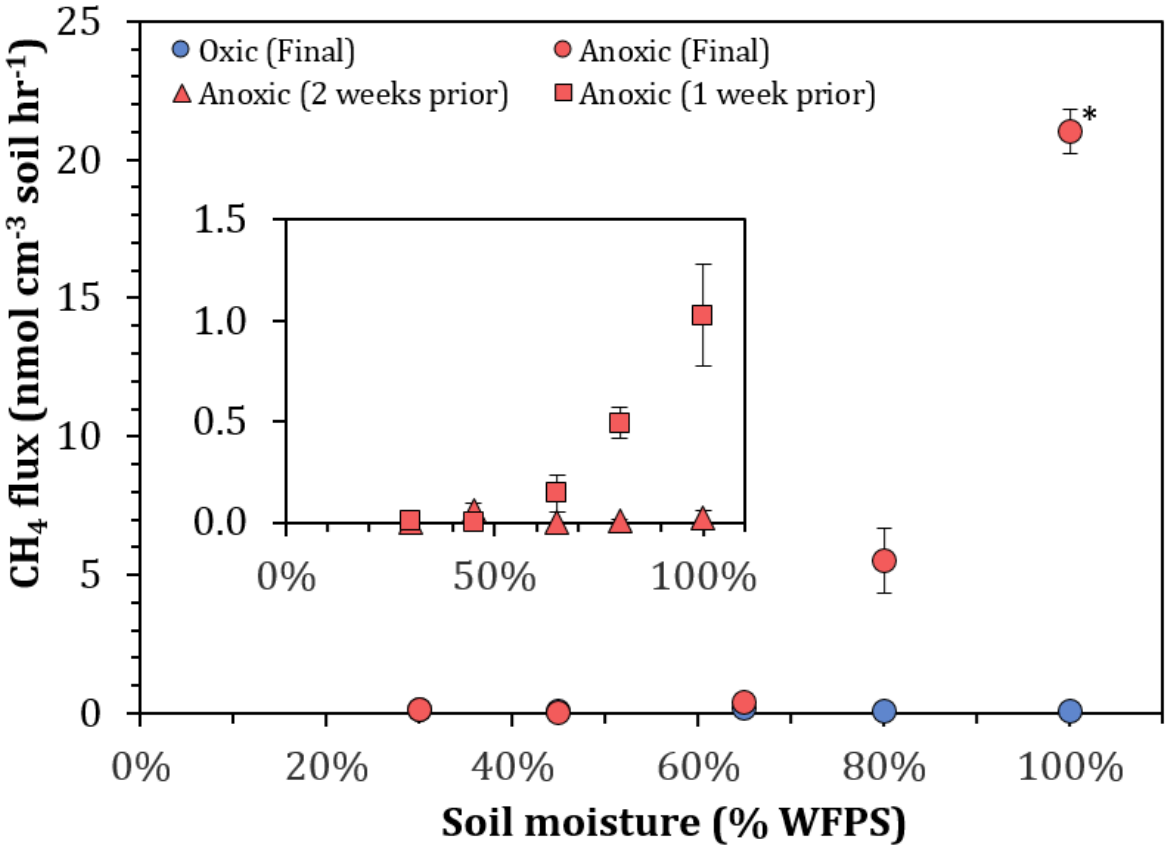

Figure 2-4: Measured CH_4 effluxes at the end of the 21-day incubations for oxic (blue circles) and anoxic (red circles) soil samples at different moisture contents with standard deviation (n=3, *n=2). Two previous timepoints for CH_4 flux measurements in the anoxic incubation are shown in the inset graph (note the smaller scale). Red squares show fluxes approximately 1 week prior to the final measurements (*i.e.* 13 days after beginning the incubation), and red triangles show fluxes approximately 2 weeks prior to the final measurements (*i.e.* 5 days after beginning the incubation).

2.3.2 Pore water geochemistry

As noted in section *2.2.3*, the pore water could not be extracted from samples of 30% and 45% WFPS and therefore the following pore water data refers only to samples of 65%, 80% and 100% WFPS. Concentrations are expressed per gram of bulk soil as a mean plus or minus standard deviation, or as a range among the 65%-100% WFPS samples. Pore water pH ranged from 7.1-7.4 in the initial samples and was not significantly different between oxic samples (range 7.0-7.5) and anoxic samples (7.0-7.2) ($p>0.05$, independent samples t-test) at the end of the incubation. Pore water EC was 0.9-1.1 mS/cm in the initial samples and was significantly higher in the anoxic

samples (2.2-2.5 mS/cm) than in the oxic samples (1.0-1.6 mS/cm) at the end of the incubation ($p<0.05$, independent samples t-test).

Pore water concentrations of NO_3^- (Figure 2-5) were high (2.30 ± 0.31 µmol g^{-1} bulk soil) in the 65% oxic sample but decreased with increasing moisture content down to 0.01 ± 0.01 µmol g^{-1} at 100% WFPS. Under anoxic conditions, NO_3^- was low in all samples measured (<0.001 µmol g^{-1}). Pore water SO_4^{2-} concentrations (Figure 2-5**)** were also low in the 100% WFPS oxic samples (0.02 ± 0.02 µmol g^{-1}) and in the anoxic samples (<0.01 µmol g^{-1}), though not as depleted as NO_3^-. Cl^- concentrations, like EC, were elevated in the anoxic samples (1.29-1.90 µmol g^{-1}) compared to the oxic samples (0.94-1.53 µmol g^{-1}). The decreasing trend of NO_3^- with moisture content in the initial samples can be explained by a dilution effect since NO_3^- was not present in the artificial soil water used to adjust the soil moisture. Conversely, for SO_4^{2-}, the increasing trend is explained because SO_4^{2-} was present in the artificial soil water but likely at a higher concentration than in the natural soil.

For the soluble organic and inorganic carbon, results are from both direct pore water extractions on the 65, 80 and 100% WFPS samples ("dissolved" fraction) and K_2SO_4 extractions on all samples ("total soluble", see *2.2.3*). Both dissolved organic carbon and the total soluble organic carbon (Figure 2-6) were greatly increased in the anoxic samples compared to the oxic samples, and among the oxic samples the 100% WFPS samples had the greatest soluble organic carbon. Both dissolved inorganic carbon and the total soluble inorganic carbon (Figure 2-6) increased with moisture content in both the oxic and anoxic samples.

Of the low molecular weight organic acids analyzed, anoxic samples had elevated concentrations of acetate, propionate and butyrate compared with oxic samples (Figure 2-7). Among the anoxic samples, acetate accumulated to concentrations up to maximums over 5700

nmol g^{-1}, propionate to over 550 nmol g^{-1} and butyrate to over 230 nmol g^{-1}. Among the oxic samples, acetate was not detectable, and propionate and butyrate concentrations were only up to maximums of 2.2 and 0.3 nmol g^{-1}, respectively. Lactate was detected at small concentrations among the oxic samples (0.9-5.1 nmol g^{-1}) but was not detected in anoxic samples. Moisture content did not have a consistent effect on organic acid concentrations within the oxic or the anoxic samples. None of the other organic acids analyzed were above detectable levels.

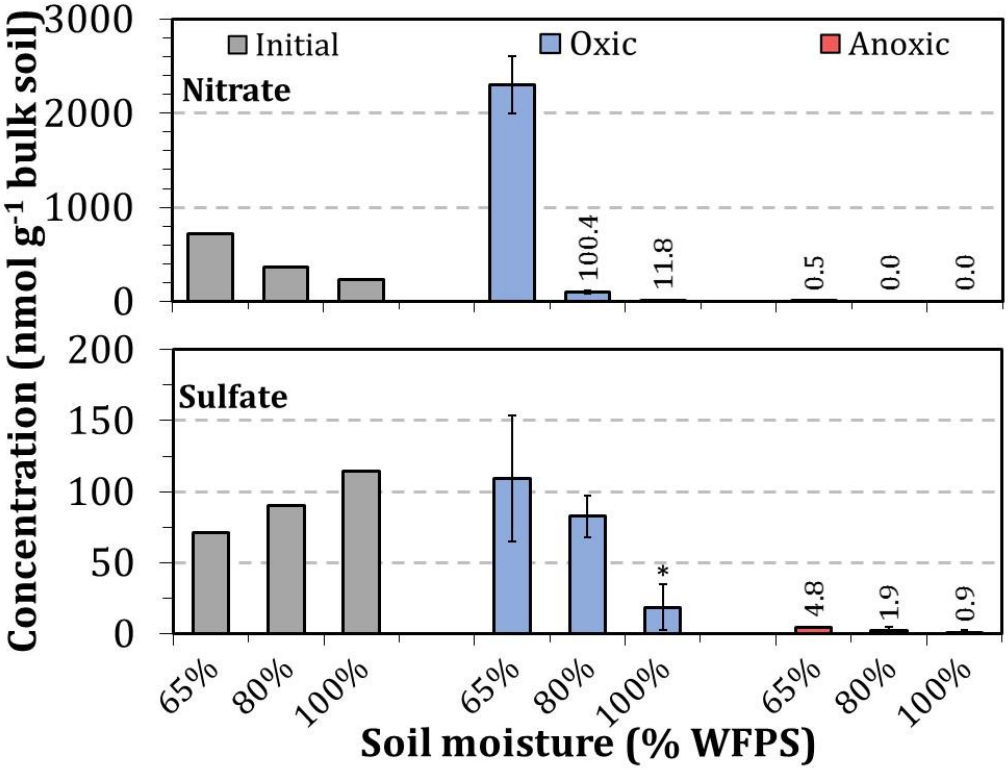

Figure 2-5: Pore water concentrations of nitrate and sulfate measured at the beginning of the experiment (initial – grey) and end (oxic – blue and anoxic – red) of the incubation for moisture contents 65%, 80% and 100% WFPS. Error bars represent standard deviation for end samples (n=3, *n=1), not shown for initial samples (n=1). Measurements were not possible for 30% and 45% WFPS moisture content samples.

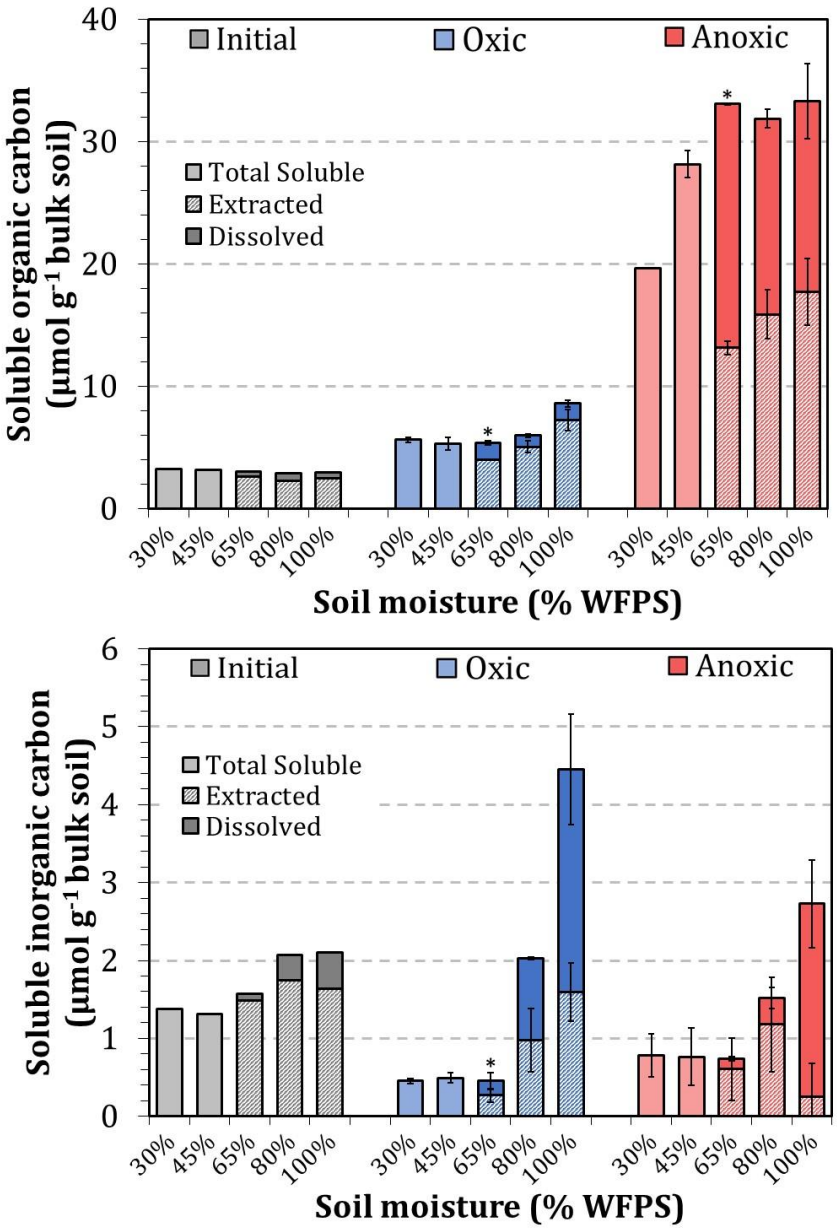

Figure 2-6: Soluble organic (top) and inorganic (bottom) carbon in soil pore water and K_2SO_4 extracts measured at the beginning (initial – grey) and end (oxic – blue and anoxic – red) of the incubation. The concentrations measured in the K_2SO_4 extracts represent the total soluble concentration (lighter shade), the concentrations measured in the pore water represent the dissolved fraction of the soluble concentration (darker shade) and the difference between these concentrations represents the extracted fraction (striped). For 30 and 45% WFPS, only the total soluble concentration was measured, whereas for 65, 80 and 100% WFPS, both total soluble and dissolved was measured and therefore the fractions are shown. Error bars represent standard deviation (n=3, *n=2), not shown for initial samples (n=1).

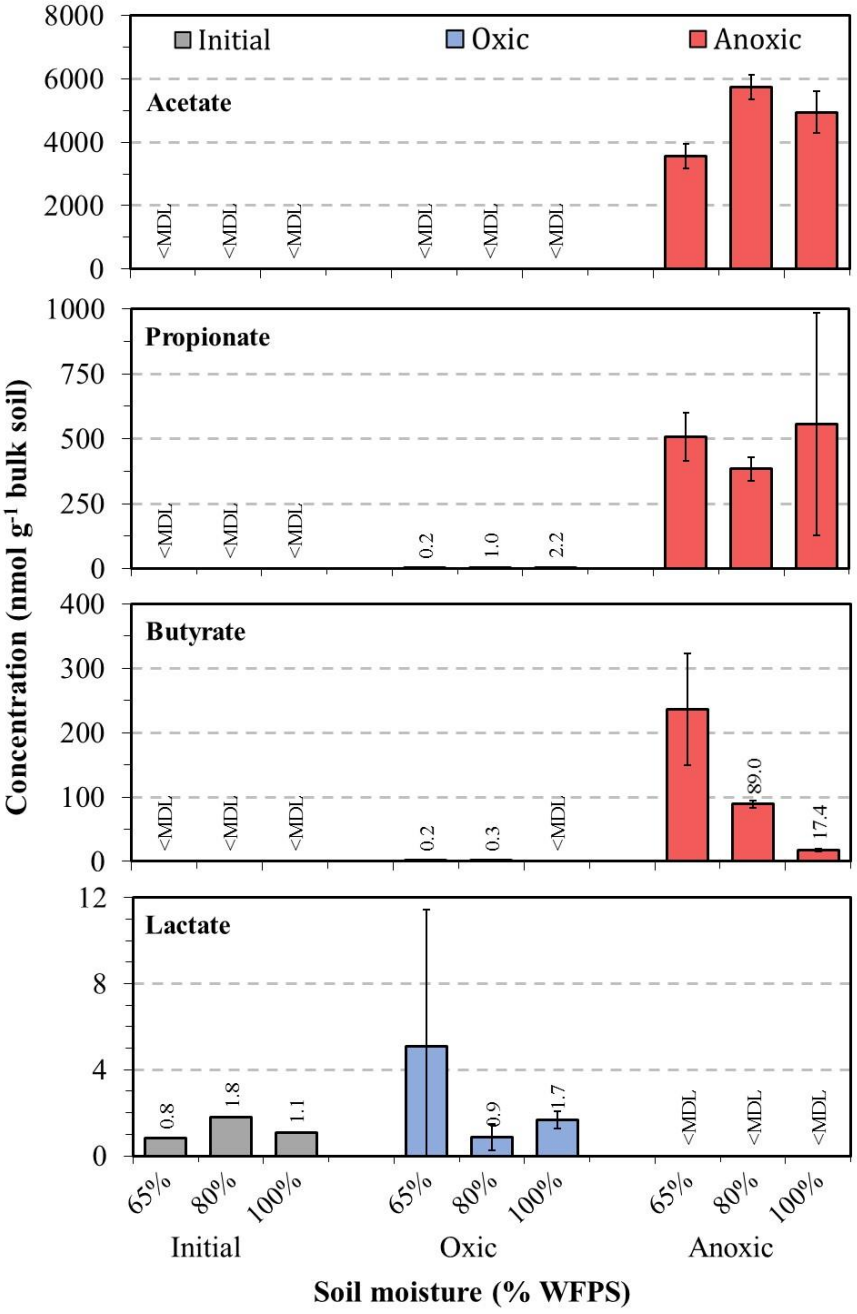

Figure 2-7: Pore water concentrations of acetate, propionate, butyrate and lactate measured at the beginning of the experiment (initial – grey) and end (oxic – blue and anoxic – red) of the incubation for moisture contents 65%, 80% and 100% WFPS. Note the different scales for each graph. Error bars represent standard deviation (n=3, except n=2 for 80% anoxic samples), not shown for initial samples (n=1). Measurements were not possible for 30% and 45% WFPS moisture content samples.

2.3.3 Model results

The CO_2 flux data in the oxic and anoxic incubations were fit with Eqs. (2.8) and (2.9), respectively (solid blue and red lines, respectively; Figure 2-3), and the residual sum of squares for the fit was calculated as 0.00026 resulting in the goodness of fit or R-squared value of 0.98. Also shown are the aerobic (dashed blue line) and anaerobic (dotted blue line) components of Eq. (2.8) where the total CO_2 flux is the sum of these two components. Values for the remaining parameters for which measurements or literature estimates were not available were estimated from this model fit (Table 2.2).

Table 2.2: Parameter values estimated by the model fit in this study

Parameter	*Value (± 95% confidence interval)*
Maximum conversion rate of aerobic reaction ($V_{max,Ox}$)	342±300 nmol cm^{-3} soil hr^{-1}
Maximum conversion rate of anaerobic reaction ($V_{max,An}$)	30±20 nmol cm^{-3} soil hr^{-1}
Half saturation constant for oxygen (k_o)	0.26±0.28 µmol cm^{-3} soil
Half saturation constant for DOC for anaerobic reaction ($k_{c,An}$)	0.44±0.13 µmol cm^{-3} soil
Eq. (2.4) exponent for oxic incubation (n_{Ox})	3.69±0.15
Eq. (2.4) exponent for anoxic incubation (n_{An})	6.5±0.2

The maximum conversion rate estimated for the aerobic respiration reaction ($V_{max,Ox}$) was about 1 order of magnitude higher than the maximum conversion rate for the anaerobic processes term ($V_{max,An}$). Additionally, the literature value of the half saturation constant for DOC in the oxic conditions ($k_{c,Ox}$) was much lower than the value estimated for that in the anoxic condition ($k_{c,An}$), although the confidence intervals for the estimates of the Michaelis-Menten parameters are relatively large. The exponent n in Eq. (2.4) was considered variable in the oxic and anoxic conditions. In the oxic condition, n was estimated to be approximately 3.7, similar to the value 3 used by Davidson *et al.* (2012), whereas in the anoxic conditions it was approximated as 6.5. This difference in the estimated n value suggests that, in addition to the greater concentration of DOC

in the anoxic conditions, the dependency of the availability of DOC on the moisture content was also greater in the anoxic incubation.

2.4 Discussion

2.4.1 Aerobic CO_2 production

Under oxic incubation, soil CO_2 fluxes followed the relationship with soil moisture that has been observed previously (*e.g.*, Linn and Doran, 1984), where fluxes were maximal at moderate soil moisture (65% WFPS) and decreased towards either moisture content extreme (30% and 100% WFPS). CO_2 fluxes were expected to become moisture-limited at low soil moisture contents due to the limited diffusion and availability of soluble substrates (*e.g.*, organic C) resulting from limited connectivity of water films within the soil (Schjønning *et al.*, 2003; Schimel, 2018). Conversely, fluxes were expected to become O_2-limited at high soil moisture contents due to the slow diffusion of O_2 in water-filled pore space, which is limiting for aerobic respiration (Ponnamperuma, 1972; Moldrup *et al.*, 2000). This relationship has been represented in soil moisture functions in CO_2 flux models, some of which use Michaelis-Menten-type kinetics (Davidson *et al.*, 2012; Moyano *et al.*, 2013).

The relationship described above is essentially a trade-off between moisture and O_2 limitations on aerobic respiration in soil. Since moisture and O_2 are closely linked in soil, few experimental studies have attempted to characterize these two factors separately. Sierra *et al.* (2017) showed that CO_2 fluxes did not decrease at high moisture contents when the O_2 concentration was held constant (at 1% or 20%), suggesting that O_2 limitation was the major factor limiting CO_2 fluxes at high soil moisture. Another experiment by McNicol and Silver (2014) demonstrated that both inundation and an anoxic headspace decreased CO_2 fluxes compared to a

moderately moist, oxic control. In our factorial experiment, the results agreed with previous studies since both anoxic incubation and saturated conditions decreased soil CO_2 fluxes. Additionally, the increasing trend observed in the anoxically incubated samples demonstrated that moisture content had an effect on CO_2 fluxes independently of O_2 availability, which could be attributed to the enhanced diffusion of soluble substrates towards the cell (and presumably, also of metabolic waste products away from the cell). Physiological limitation of low water potential may also plays a role at very low moisture contents (Schimel, 2018).

One observation of the CO_2 fluxes under oxic incubation worth noting was that fluxes did not decrease to zero at saturation, as many existing models would predict. The earlier models (*e.g.*, Davidson *et al.*, 2012; Moyano *et al.*, 2013) assume the complete absence of O_2 in saturated soils and therefore, since only aerobic respiration is represented in these models, they predict a complete inhibition of CO_2 production. In fact, previous lab incubation studies have shown non-zero fluxes of saturated soils (Moyano *et al.*, 2018; Wickland and Neff, 2008). There are two possible reasons to explain CO_2 fluxes observed in saturated soils. First, even in completely saturated soils, O_2 diffusion will occur at the soil-atmosphere interface. This allows for aerobic respiration at the interface which matches O_2 diffusion rates and therefore non-zero CO_2 fluxes. If the rate of O_2 consumption is lower than the rate of O_2 diffusion, for instance due to limited availability of labile OM, then oxic pore water will exist allowing for aerobic respiration and CO_2 production to occur. Entrapped air in saturated soil could also increase the rates of O_2 entering the soil water (Williams and Oostrom, 2000). Second, even under the complete absence of O_2, anaerobic metabolisms in the soil can produce CO_2. The CO_2 fluxes measured in the anoxic incubations indicated that this was occurring, and fluxes of CO_2 have also been reported in previous anoxic soil incubation experiments (Moore and Dalva, 1997).

2.4.2 Anaerobic CO_2 production

In addition to aerobic respiration, CO_2 is also a product of several types of fermentation and anaerobic respiration which occur in the absence of O_2. The production of low molecular weight organic acids via fermentation pathways supplies substrates for methanogens (Herndon *et al.*, 2015). Elevated DOC and organic acids, mostly acetate, suggested that fermentation was occurring in the anoxic conditions which could both produce CO_2 and fuel methanogenesis. The exhaustion of available electron acceptors is generally required for methanogenesis to occur (Knorr and Blodau, 2009). In the anoxic conditions, SO_4^{2-} and NO_3^- were almost entirely depleted by the end of the experiment, suggesting that methanogenesis would have been permitted. Other possible EAs (*e.g.,* Fe^{3+}, Mn^{4+}) were not measured in this study and therefore it was unknown how much they contributed to the cumulative anaerobic respiration.

Substantial CH_4 fluxes measured in the anoxic conditions indicate that methanogenesis was likely the main anaerobic pathway being used at the end of the experiment. However, CH_4 fluxes were dynamic over time and much smaller fluxes were observed earlier in the incubation. Since this study did not include measurements of CH_4 concentrations in the pore water, we cannot rule out the possibility that dynamic fluxes of CH_4 over time resulted from physical effects. Previous work on CH_4 emissions from peatlands has shown that CH_4 accumulates and can become supersaturated in pore water leading to the formation of gas phase CH_4 in bubbles (Strack *et al.*, 2005). Ebullition of CH_4 accumulated in bubbles can lead to high spatial and temporal variability in CH_4 emissions from soil (Tokida *et al.*, 2005) and may explain the high CH_4 flux rates at the end of the anoxic incubation in this study.

Nonetheless, the delay in CH_4 fluxes may be better explained by a lag time in methanogenesis due to inhibition by the presence of alternative EAs. For methanogenesis to

become favourable, EAs present in the soil initially would need to become depleted (through their reduction coupled to the oxidation of OM, *i.e.* anaerobic respiration). As noted above, NO_3^- and SO_4^{2-} were initially present in the pore water, and thus would have inhibited methanogenesis initially, but became depleted in the anoxic conditions by the end of the incubation. Stoichiometrically, under strictly EA-limited conditions where methanogenesis is the only available metabolic pathway, we would expect a theoretical ratio of CO_2:CH_4 produced (or HCO_3^-:CH_4) of 1:1 (*e.g.*, from the disproportionation reaction with glucose; LaRowe and Van Cappellen, 2011):

$$C_6H_{12}O_6 + 3H_2O \rightarrow 3CH_4 + 3HCO_3^- + 3H^+. \quad (2.10)$$

With the ongoing occurrence of anaerobic respiration using EAs, we would expect a CO_2:CH_4 ratio of greater than 1. Theoretically, as EAs are depleted over time and methanogenesis starts to make up greater proportions of the overall decomposition of OM, we would expect a decreasing ratio. Previous incubation experiments have observed this decline in CO_2:CH_4 over time associated with a lag in methanogenesis (Chowdhury *et al.*, 2015; Gao *et al.*, 2019). Recent work by Gao *et al.* (2019) observed declining CO_2:CH_4 ratios from incubating peat soils that reached as low as 1:1. Therefore, although we cannot say for certain if the observed CH_4 fluxes in our incubation were representative of the actual instantaneous rate of CH_4 production, previous observations have demonstrated that the development of strictly methanogenic conditions can result in equimolar production of CO_2 and CH_4.

The unsaturated soil samples incubated under oxic conditions clearly had higher CO_2 fluxes than under anoxic conditions due to aerobic respiration (Figure 2-3). The CO_2 flux at 100% WFPS was very similar under both oxic and anoxic incubations, suggesting that much of the CO_2 produced under saturation results from anaerobic processes rather than aerobic respiration at the

soil-headspace interface. However, measurable CH_4 fluxes were not observed in any of the oxic incubations, even under completely saturated conditions (Figure 2-4). This could have been due to the presence of an aerobic headspace and the possible oxidation of any produced CH_4 by methanotrophs in oxic upper layers of the soil, which would also contribute to CO_2 fluxes (Boucher *et al.*, 2009). Alternatively, methanogenesis may not yet have been occurring in these samples due to the availability of EAs. Decreases in SO_4^{2-} and NO_3^- concentrations suggested that some reduction of these EAs was occurring, especially in the highest moisture contents, but they were not completely depleted by the end of the incubation as in the anoxic incubations (Figure 2-5). Additionally, organic acids such as acetate did not accumulate in the oxic samples as they did in the anoxic samples (Figure 2-6), suggesting that the presence of EAs may have inhibited fermentation and thus organic acid substrates for methanogenesis were not being supplied. Alternatively, organic acids may have been quickly respired aerobically and thus did not accumulate. Therefore, anaerobic respiration pathways such as denitrification or SO_4^{2-} reduction (or the use of other inorganic or organic EAs that were not measured) may have been the main anaerobic source of CO_2 in the oxic incubations rather than fermentation and methanogenesis.

2.4.3 Modelling CO_2 fluxes

The experimental results highlighted the importance of including anaerobic sources in soil CO_2 flux models. The model developed here represents a simple way of incorporating these anaerobic processes as a lumped term into existing soil moisture functions which could eliminate much of the model-data discrepancies often observed at the high end of soil moisture content. However, as discussed above, multiple pathways exist for anaerobic CO_2 production and thus, representing them as one bulk process was an oversimplification. For the purposes of this study, the lumped term was deemed appropriate since there was insufficient data to estimate the exact

contributions of individual metabolisms, but future studies may find it useful to quantify additional reaction rates. Time scales are also important to consider since availability of EAs will be temporally dynamic. For example, O_2 and other electron acceptors that are initially present upon flooding of soil will eventually become depleted if they are not replenished (Parsons *et al.*, 2013; Rezanezhad *et al.*, 2014). Therefore, multiple metabolisms may be used transitionally under dynamic soil moisture conditions and more complete models could explicitly represent these metabolisms (Zheng *et al.*, 2019).

As mentioned, non-zero CO_2 fluxes from saturated and anoxically incubated soils have been observed before. In a different approach to dealing with this discrepancy than how we have described here, Ghezzehei *et al.* (2019) attributed non-zero fluxes at saturation to a minimum level of aerobic respiration in their model. The Terrestrial Ecosystem Model (Raich *et al.*, 1991) similarly includes a soil moisture function which has a parameter for the rate of decomposition at saturation which is 60-80% of the maximum rate. However, the substantial CO_2 fluxes in anoxic conditions in this experiment suggest that anaerobic sources likely explain more of the saturated fluxes than aerobic respiration.

Applying this type of soil moisture function to models that operate on a batch experiment or field scale is additionally challenging since bulk soil moisture measurements are not necessarily representative of soil moisture and O_2 distribution at the pore and aggregate scales (Keiluweit *et al.*, 2018). Anoxic microsites in under-saturated soils have been increasingly recognized as an important factor for soil C decomposition (Keiluweit *et al.*, 2017; Brewer *et al.*, 2018), and models will be required that account for this microscale heterogeneity (Ebrahimi and Or, 2016). This model's representation of O_2 inhibition of anaerobic respiration as a function of moisture content allowed for this heterogeneity instead of having a strict limit for complete inhibition at a certain

threshold of O_2 availability, but the reality is of course more complex. Additionally, understanding the roles of soil properties (*e.g.,* soil texture, OM content) will be critical for the development of models that can accommodate a range of soil types (Keiluweit *et al.*, 2018; Ghezzehei *et al.*, 2019; Tang and Riley, 2019).

2.4.4 Conclusion

There is a need to develop soil moisture functions that are conceptually accurate for CO_2 fluxes. The factorial design of the experiment in this study allowed us to look at the effects of soil moisture and O_2 on soil CO_2 fluxes independently. Under oxic conditions, both moisture and O_2 were controlling factors, whereas under anoxic conditions, only moisture was a controlling factor as O_2 was consistently absent. The different relationships of CO_2 fluxes with soil moisture under both oxic and anoxic conditions are evidence of the trade-off between moisture and O_2 limitations in soil that has long been assumed but rarely validated. The findings also highlighted the importance of considering anaerobic processes as sources of CO_2. The model-data discrepancy that has been observed in high soil moisture CO_2 fluxes can be explained by the lack of consideration of these anaerobic processes. This relatively simple model presents an overlooked component of soil CO_2 fluxes that can be incorporated into increasingly complex, mechanistic models for soil C decomposition.

3 Interactions between soil texture and soil moisture in controlling CO_2 fluxes: Literature review and batch experiment

3.1 Introduction

In Chapter 2, I investigated how soil moisture and oxygen (O_2) influence soil CO_2 fluxes using a batch incubation experiment and presented an improved way of representing this relationship in models. The goal of many soil organic matter (OM) decomposition models is to accurately scale up micro-scale biogeochemical processes to predict global carbon (C) transformations. While the previous chapter addressed soil moisture as a key factor controlling soil CO_2 emissions, one factor I did not consider was how this effect could change depending on intrinsic soil properties. A robust model that accurately predicts rates of CO_2 fluxes from soil will need to consider the differences in intrinsic properties between soils that can affect OM decomposition or interact with other factors controlling soil OM decomposition processes.

Soil texture is one factor that can vary widely between different soil types and influences the rates of OM decomposition in soil. Clay content, for example, can reduce rates of soil organic C turnover by protecting OM from decomposition (Hassink, 1997). Mechanisms that control the protection of soil OM include spatial inaccessibility (*e.g.,* through occlusion within aggregates or intercalation within phyllosilicates) and interactions with particle surfaces (Lützow *et al.,* 2006). By directly or indirectly providing a protective effect on soil OM, clay content may act as a controlling factor for soil CO_2 fluxes. Some existing models explicitly include clay content as a parameter for the prediction of OM decomposition rates (*e.g.,* Sulman *et al.,* 2014).

In addition to protecting soil OM, soil texture may affect the relationship between soil CO_2 fluxes and soil moisture. Some models hypothesize that soil clay content can shift the moisture content where maximum fluxes occur, or modify the shape of the curve that represents this relationship (see Figures 3-1 to 3-3; Moyano *et al.,* 2013; Ghezzehei *et al.,* 2019; Tang and Riley,

2019). Moyano *et al.* (2012) provided some support for this hypothesis by synthesizing and analyzing data collected from a wide range of soils. However, very little experimental evidence exists to test this prediction or investigate the exact mechanisms involved. More experimental studies using direct manipulation of soil texture will be useful for validating the proposed conceptual models and testing further hypotheses regarding the mechanisms involved.

The purpose of this chapter is to identify a possible area of future research, that is, the effects of soil texture on soil CO_2 fluxes and their relationship with soil moisture, and to provide an overview of the current state of knowledge on this topic. Some previous studies using different methodologies are discussed in this review. Additionally, a review of some existing models is presented to identify some existing frameworks that consider soil texture and its effect on organic matter decomposition or CO_2 fluxes. Finally, I present the results of a factorial batch experiment conducted to examine the interaction between soil texture and soil moisture and the effects on soil CO_2 fluxes.

3.2 The role of soil texture in soil organic matter dynamics

3.2.1 Findings from previous experimental studies

Effects of clay content on OM stabilization

The effects of soil clay content on the stabilization of soil OM were introduced in Chapter 1 in this thesis. In brief, increasing clay content increases OM stabilization, thereby reducing emissions of CO_2. One mechanism by which the presence of clay minerals can protect soil OM from decomposition is by adsorbing molecules of OM or otherwise directly interacting with OM. The factors that can influence this protective effect include the clay content, clay type (2:1 vs. 1:1) and clay size fractions (Six *et al.*, 2002). For example, as a 1:1 clay, kaolinite has a lower cation exchange capacity and less capacity to adsorb OM than 2:1 clays such as smectites or illites (Barré

et al., 2014). Sørensen (1972) demonstrated that while adding either montmorillonite or illite to soil significantly increased OM protection, the addition of kaolinite had no stabilizing effect. Saidy *et al.* (2012) also showed that dissolved OM decomposition in soil was greater in the presence of kaolinite than illite or smectite. Therefore, while some models have estimated OM protection using clay content, other factors such as the clay type and mineralogy are important to consider as well.

Clay content indirectly influences OM protection because clay minerals are a key component of microaggregate formation (Totsche *et al.,* 2018). Microaggregates are stable structures in the soil with micropores that can influence soil tortuosity, water retention, and effective diffusion rates (Zhuang *et al.,* 2008). Soil OM entrapped within microaggregate structures is physically protected from decomposition due to spatial inaccessibility (Chenu and Plante, 2006). In addition to physical occlusion, microaggregates can also limit OM decomposition by limiting O_2 diffusion. A study by Sey *et al.,* (2008) demonstrated that O_2 diffusion was more restricted within microaggregates than macroaggregates. Therefore, it can be expected that soil texture influences the degree of O_2 limitation in soil, and a study by Keiluweit *et al.,* (2018) supported this by showing that the overall volume of anoxic microsites in a soil increased with clay content.

Interactive effect between soil texture and moisture: experimental approaches

Of the studies that have investigated the effects of soil texture on OM decomposition in soils, some have done so using soil samples from sites with natural gradients in soil texture (Sørensen, 1975; Gregorich *et al.,* 1991; Amato and Ladd, 1992; Schjønning *et al.,* 2003) . While these studies were able to use natural, undisturbed soil samples that were likely more representative of field conditions, they may have been disadvantaged due to uncontrolled variation in soil properties other than the property of interest to the study. For example, natural gradients in soil texture can also be associated with gradients in OM content (Burke *et al.,* 1989). Although OM decomposition

rates can be normalized to the amount of OM in each treatment, deciphering the interactive effects of soil texture and other factors (*e.g.,* soil moisture) is challenging. Others have attempted to increase the level of control by adding different proportions of specific grain size fractions to manipulate soil texture directly. This has been done using commercially available pure clay and sand (Sørensen, 1972; Kunc and Stotzky, 1974) and with clay and silt particle size fractions collected from a natural soil (Schjønning *et al.,* 1999; Thomsen *et al.,* 1999). Another approach is to use an artificial soil for which soil mineralogy, OM content and texture are controlled, and which must be inoculated with, for example, a natural soil community (Pronk *et al.,* 2013).

While many previous studies have investigated the effect of clay content on soil OM decomposition, few experiments have looked at the possible interactions between soil texture and soil moisture in controlling soil CO_2 fluxes. Soil texture could affect OM decomposition and other processes in soil by influencing the diffusion of substrates to and waste products away from the microbial cells. Soil texture has been shown to be an important factor that influences gas transport in soils (Dörr *et al.,* 1993). Keiluweit *et al.* (2018) showed that the volume of anoxic microsites in moderately moist soil varied depending on soil texture, demonstrating the link between clay content and diffusive limitations on O_2 availability in soil. Soil texture can also affect the diffusion of soluble substrates such as DOC, for example, due to tortuosity effects (Moldrup *et al.,* 2001), which has been shown to limit microbial activity at low soil moisture contents (Schjønning *et al.,* 2003). A flow-through reactor experiment in a study by Rezanezhad *et al.,* (2016) showed that increasing the proportion of sand in peat-sand mixtures increased the rate of denitrification normalized to the mass of organic C, demonstrating the importance of transport properties to OM decomposition by denitrification in peat soil. Since soil texture plays a role in controlling diffusive

availability of both soluble substrates and gases such as O_2, it should be expected that soil texture can influence the soil CO_2 flux-moisture content relationship.

An experiment by Scott *et al.* (1996) assessed OM decomposition rates in different soils having a natural gradient in soil texture and at different soil water pressures. While they did not observe a significant effect on OM decomposition by soil texture alone, the effect of soil moisture on OM decomposition was most pronounced in the finer-textured soil. This provided some evidence for an interactive effect between soil moisture and soil texture; however, the differences in soil organic C content between soil textures in the natural gradient make it is difficult to assess the reason for the interaction.

Experiments by Thomsen *et al.* (1999) tested both a natural gradient in soil texture, and soil textures adjusted artificially by adding clay size fractions that had been extracted from the natural soil. They suggested that soil texture can indirectly affect decomposition rates due to its effect on soil water characteristics. However, results from the natural gradient versus the adjusted soil textures were inconsistent, possibly because the OM added with the clay size fraction may have been more recalcitrant compared with the bulk soil OM, resulting in differences in overall soil OM quality. While these experiments may have been more realistic by adjusting soil texture with clay and silt sized particles extracted from the natural soil, the additional OM added this way introduced additional variability into the clay and silt-content treatment groups. The alternative, adding pure clay, may not ensure consistent mineralogy with the natural soil but the OM quantity and quality could be better controlled.

3.2.2 Existing modelling frameworks

Up until very recently, most models did not consider how soil texture could influence the relationship between soil moisture and CO_2 fluxes. While some more recent models have provided a conceptual framework for this possible interactive effect, these models have had little direct experimental evidence available to verify their assumptions and test hypotheses regarding the exact mechanisms involved. Still, a discussion of these existing models is useful, since they provide a framework for starting to develop hypotheses based on theoretical concepts and established empirical relationships.

The Terrestrial Ecosystem Model (Raich *et al.*, 1991) has been used to predict net primary productivity and C fluxes at the continent and global scales. The soil moisture function used to scale estimates of soil OM decomposition rates could be changed to reflect the soil texture. Parameters for the optimum soil moisture were defined for 5 soil texture classes based on the soil moisture at which 15% of the soil volume is air. According to this assumption, the soil moisture content at which OM decomposition is maximized increases with increasingly fine-textured soil. While early models such as the Terrestrial Ecosystem Model identified the need to modify soil moisture sensitivity according to the soil texture, more recent models have introduced increasingly mechanistic rationale for these relationships.

The DAMM model (Davidson *et al.*, 2012) and other similarly formulated models estimated the relative gas diffusivity in soil compared to free air by relating it to the air-filled pore space. For example, the relationship in the DAMM model was based on the following relationship (Moldrup *et al.*, 2000):

$$D_p/D_o = \varepsilon^{4/3}, \tag{3.1}$$

where D_p/D_o is the relative gas diffusivity in soil and ε is the volumetric air-filled porosity, and *4/3* represents a pore-connectivity factor. More recently, studies have shown that this pore-connectivity factor relates to the soil particle and pore size distribution (Arthur *et al.*, 2012). While it might be assumed that soils with greater porosity (*i.e.* lower bulk density) would have greater D_p/D_o due to greater pore volume, denser soils actually exhibit greater D_p/D_o due to increasing proportion of effective pore volume (Fujikawa and Miyazaki, 2005). This may further explain the results of Keiluweit *et al.*, (2018) where increasing clay content increased the volume of anoxic microsites, since a greater proportion of inaccessible micropores would limit O_2 diffusion. Therefore, the relationship between soil texture and effective porosity may be important in controlling gas diffusion in soil.

A model by Moyano *et al.* (2013) used empirical relationships relating the gas and solute diffusivities to soil texture characteristics. For example, the relative solute diffusivity ($D_s/D_{o,s}$) was related to a threshold soil moisture level (θ_{th}) through the relationship established by Olesen *et al.*, (2001):

$$D_s/D_{o,s} = 1.1\theta(\theta - \theta_{th})\,. \tag{3.2}$$

Moldrup *et al.*, (2001) empirically related θ_{th} to the soil surface area, and thus the soil texture, by:

$$\theta_{th} = 0.039\ {SA_{vol}}^{0.52}, \tag{3.3}$$

where SA_{vol} is the volumetric soil surface area. Using these empirically derived relationships, Moyano *et al.* predicted that the relationship between relative microbial respiration and water saturation changes depending on θ_{th}, with greater values of θ_{th} resulting in a narrower peak (Figure 3-1).

In their soil heterotrophic respiration model, Yan *et al.* (2018) defined two parameters that describe the relationship between soil moisture and CO_2 fluxes: a parameter related to the degree

of collocation of the soil OM and microorganisms, and a parameter related to the restriction in O_2 supply. By fitting their model to experimental data from a range of soil textures, they found that the SOC-microorganism factor was positively and linearly related to clay content (Figure 3-2A). They suggested the reason for this is the adsorption of OM on clay particles or the occlusion of OM within aggregates, which makes the OM inaccessible to the microbes. The graph in Figure 3-2B shows how relationship between relative water content and relative respiration rate changes if the SOC-microorganism collation factor (represented as *a* in the figure) is increased. Conversely, they found that the O_2 supply restriction factor was not correlated with soil properties, which was surprising given past experimental evidence suggesting that O_2 supply is influenced by clay content (*e.g.*, Keiluweit *et al.*, 2018).

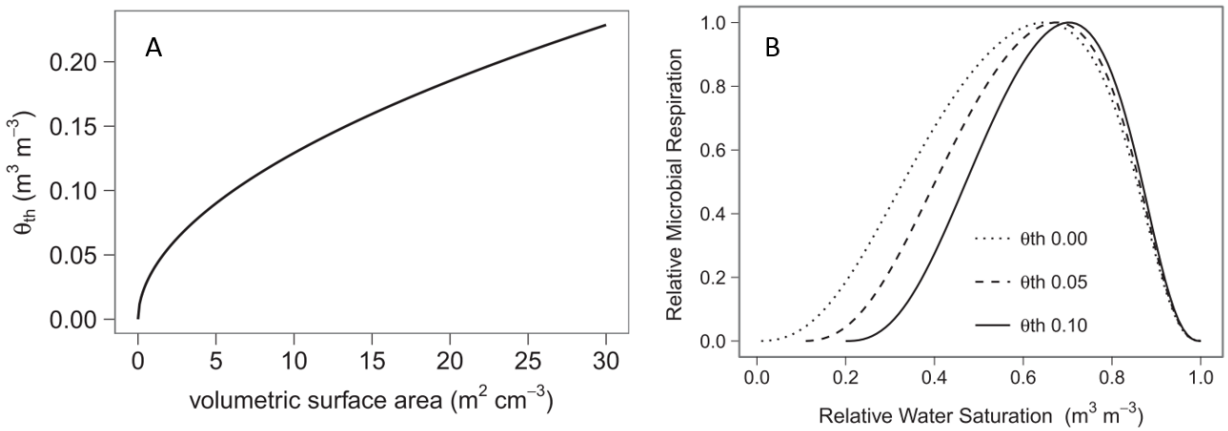

Figure 3-1: Figures obtained from Moyano *et al.* (2013) showing their model predictions that (A) the threshold soil moisture content (θ_{th}) depends on the volumetric surface area (which is linked to the soil texture), and (B) the relationship between relative respiration and water saturation depends on θ_{th}.

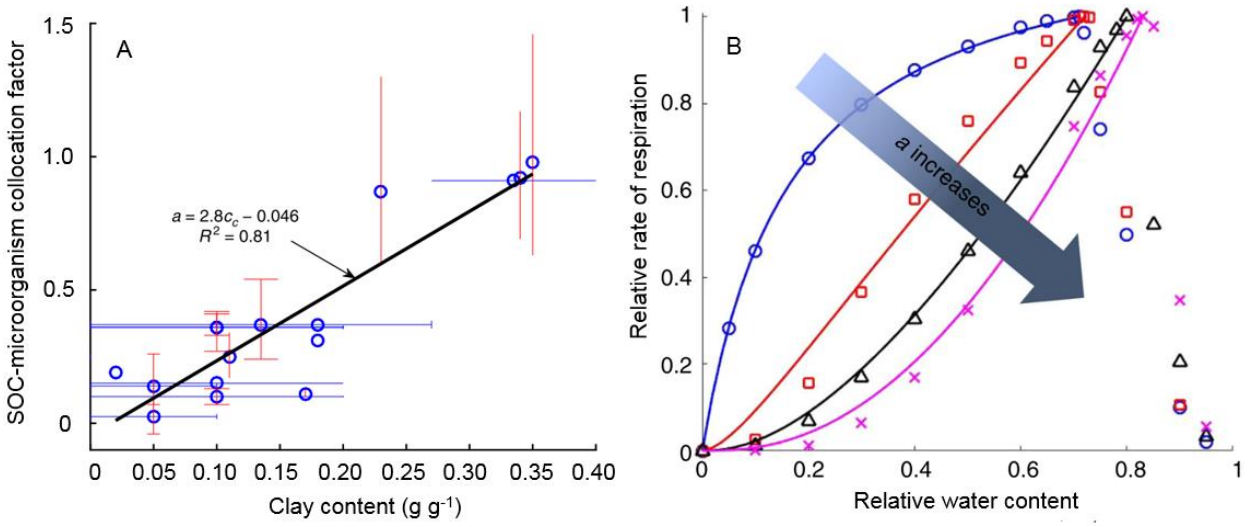

Figure 3-2: Figures obtained from Yan *et al.* (2018). Panel A shows the fitted values from for the SOC-microorganism collocation factor (*a*) correlated with clay content. Panel B shows how changing the value of this parameter influenced the relationship of relative water content with the relative rate of respiration.

The approach taken by Ghezzehei *et al.*, (2019) to include soil type-specific properties in their model was to incorporate parameters relating to the soil water characteristic, or soil water retention curve. The soil water characteristic is a well-established relationship between soil water content and matric potential (Van Genuchten, 1980) and is a bulk-soil scale representation of the pore properties and distribution. Thus, by including soil water characteristic parameters, their model could account for differences in water retention and transport due to soil texture. The use of the soil water characteristic was made even more accessible by pedotransfer functions which allowed for estimation of the parameters using routinely measured soil properties such as the particle size distribution (Zhang and Schaap, 2017). Using their model that considers the dependence of substrate and O_2 diffusion on soil matric potential in conjunction with a pedotransfer function, they predicted that soil texture impacts soil moisture sensitivity. Their model predicted that fine-textured soils have a wider range of soil matric potential where peak CO_2 fluxes occur and coarse-textured soils have a narrower range (Figure 3-3A). However, when

soil moisture was expressed as relative saturation (as opposed to matric potential), it was the fine-textured soils that exhibited the narrower range (Figure 3-3B).

Another modelling framework that included the use of pedotransfer functions was developed by Tang and Riley (2019). Their model estimated many parameters *a priori* using numerous mechanistic or well-established empirical relationships to calculate effective affinity parameters used in kinetic models of OM decomposition, including Michaelis-Menten kinetics. They used a pedotransfer function to estimate the matric potential at a given moisture content using a parameter for pore size distribution. They then estimated the solute and gas diffusivities based on the thickness of water films around soil particles, which they calculated based on the matric potential. In this way, they could use soil texture (*i.e.* clay content) to determine the relative soil moisture sensitivity. They reported their model results based on relative saturation and their model predicted that the range of optimum moisture content becomes narrower with increasing clay content (Figure 3-4). The effect appeared most pronounced at low soil moisture, as it did in the model predictions of Ghezzehei *et al.* (2019).

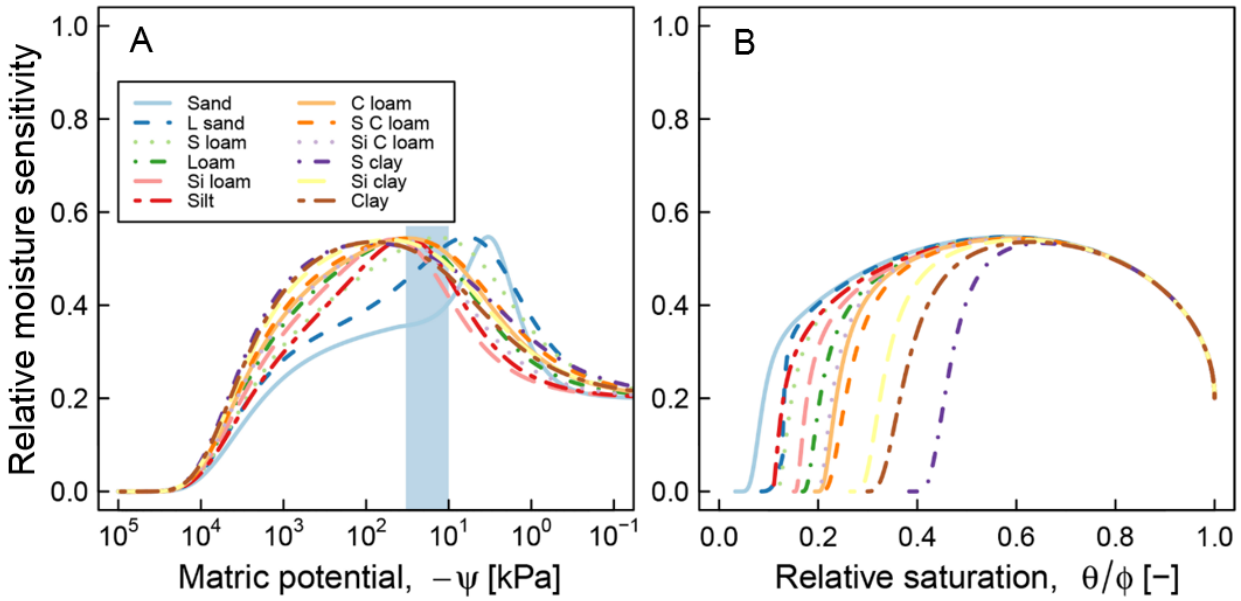

Figure 3-3: Figures obtained from Ghezzehei *et al.* (2019) showing their model predictions for the effect of soil texture class on the relative soil moisture sensitivity of aerobic respiration activity. Soil moisture was expressed as matric potential (A) and as relative saturation (B). Their model used soil water characteristic parameters estimated from the soil texture classes using a pedotransfer function.

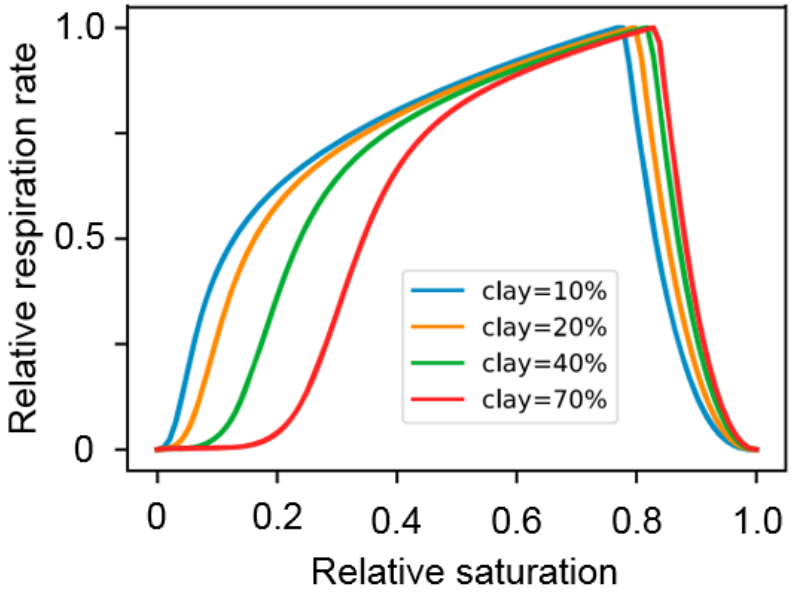

Figure 3-4: Figure obtained from Tang and Riley (2019) that shows their model predictions for the effect of clay content on the relationship between relative respiration rates and relative saturation.

3.3 Factorial batch experiment

While reviewing the literature on developments in modelling soil OM dynamics and CO_2 fluxes involving soil texture, it became clear that little experimental evidence exists to validate the assumptions made in current models. I therefore developed an experimental set up to directly test effects of both soil moisture and soil texture on CO_2 fluxes using a factorial batch incubation experiment. While factorial experiments investigating both soil texture and soil moisture have been rare, there have been some previous efforts to investigate soil texture as a factor controlling OM decomposition in soil. Among the different approaches to testing different soil textures discussed above, I chose the method of adding pure clay and sand to prepare soils of varying textures. This method allowed for a high level of control (*i.e.,* other factors are kept constant among the different treatments) while still using a natural soil.

3.3.1 Materials and methods

Soil collection and preparation

Soil for this experiment was collected from an agricultural field at the *rare* Charitable Research Reserve in Cambridge, Ontario (the same location as described in Chapter 2, Figure 2-1) in July 2019. At the time, the field was planted in corn and in previous years it was rotated in soy, corn and wheat and red clover. Collected soil was sieved to 4 mm, air dried for 1 week and then stored at 4°C for approximately 3 months until the experiment was started. A commercially available composted cattle manure (GardenClub™) used to amend the soil was also similarly sieved and air-dried.

Different soil textures were prepared by adding pure kaolinite clay (Kaolinite, natural, Sigma-Aldrich), pure quartz sand (3Q-ROK®, US Silica), or a mixture of both to the agricultural

soil amended with composted cattle manure. As a comparatively inert clay, kaolinite was chosen for soil texture adjustment to minimize effects related soil OM adsorption so that any observed differences could be attributed to soil texture differences rather than mineralogy. Three soil compositions were prepared for the incubation experiment: Texture 1, Texture 2 and Texture 3, corresponding to soil compositions increasing in their proportions of fine particles (silt + clay). The 3 soil compositions (Figure 3-5) were prepared according to the compositions shown in Table 3.1 and well-mixed. Particle size distributions of the agricultural soil and the 3 soil compositions (Table 3.1) were analyzed using the pipette method (Gee and Bauder, 1986). Gravimetric moisture content was also measured for the 3 soil compositions by oven-drying at 105°C for 24 hours (Gardner, 1986).

Table 3.1: Composition and particle size analysis of prepared soils (% mass)

Component	*Agricultural soil*	*Texture (1)*	*Texture (2)*	*Texture (3)*
Agricultural soil		40	40	40
Composted manure		10	10	10
Quartz sand		50	37.5	25
Kaolinite clay		0	12.5	25
Sand	48.8	75.3	63.9	48.1
Silt	39.5	17.9	24.1	32.0
Clay	11.7	6.8	12.1	19.9
Silt + clay	51.2	24.7	36.2	51.9
Texture class	Loam	Sandy loam	Sandy loam	Loam

Among the different soil textures prepared, the amended agricultural soil made up the same proportion by mass of each soil mixture. The remaining fraction of the soil mixtures were made up of a mixture of kaolinite clay and quartz sand, the proportions of which were varied to achieve different overall soil texture. In this way, the dilution of the natural soil with pure minerals was the same for each treatment, thus keeping many important factors consistent across treatments

(*e.g.*, OM content, biomass). The same amount of composted cattle manure was added to each soil type to maintain an OM content similar to that of the natural soil before dilution.

Allocations of 200 g of the mixed soils were weighed into 500 mL glass jars (soil surface area: approximately 35 cm^2). Triplicate soil samples were prepared for each treatment combination, which included the 3 soil textures and 8 moisture content levels for a total of 72 samples. Moisture contents of the soil samples in jars were adjusted with water prepared to closely match the pH, electrical conductivity and ionic composition of the groundwater from the field site (composition outlined in section *2.2.1*). As in the Chapter 2 experiment, an artificial soil water was used for moisture content adjustment rather than pure water so as to minimize disturbances to the soil community due to osmotic or pH shock (Killham, 1985; Halverson *et al.*, 2000). The first samples to be adjusted were those that were designated to be 100% saturated. To achieve this, water was added slowly and the soil mixed until complete saturation was achieved. The same amount of water was added to saturate the soils of Texture 1 and Texture 2 (47.6 mL), but a larger volume of water was needed to fully saturate the soils of Texture 3 (60.0 mL). Sequentially smaller volumes of water were added to the remaining soils to achieve moisture contents ranging from fully saturated (100% WFPS) to no water added (approximately 7% WFPS, due to residual moisture in the soil). The soil samples were well-mixed to evenly distribute the water and then packed down to approximately equal volumes (small differences in volume were recorded and accounted for in bulk density and headspace volume calculations, with Texture 3 generally having lower bulk densities than the other two soil textures).

Figure 3-5: Photos of (A) prepared soil types before moisture adjustment (left to right, soil textures increasing in proportion of silt+clay: Texture 1 – Texture 2 – Texture 3), and (B) all soil sample jars after soil moisture adjustment and during gas flux measurements.

Incubation experiment and gas flux measurements

Soil moisture adjustment was carried out over 3 days, with the first replicate of each treatment being prepared on the first day, the second on the following day and the third on the third day. Incubations began on the day that the soil moisture was adjusted for each sample, thus, since preparations were staggered over 3 days, measurements were also staggered over 3 days such that the amount of time between the beginning of the incubation and any measurements was equal for each set of replicates. The purpose of staggering incubations was to limit the number of samples that needed to be analyzed on a given day, since the large number of samples introduced logistical challenges for measuring gas fluxes. The scheduling of the gas flux measurements therefore involved measuring fluxes from 24 samples per day, and repeated measurements on the same soil sample were at minimum 3 days apart. The incubations were completed after 20 days.

Samples were incubated in a walk-in environmental chamber (Percival Scientific CTH-118) at 25°C ±1°C so that gas flux measurements would not be affected by changes in temperature, which is another major factor controlling soil CO_2 fluxes. Samples were incubated in glass jars

with lids fitted with ports for gas sampling. Lids were left on during the incubation but the ports were open; thus, the jars were not sealed but limited air exchange minimized evaporation from the soil samples. Soil samples were weighed approximately every 3 days (on the day following a gas flux measurement) and topped up by misting with MilliQ ultrapure water to replace any water lost to evaporation. Typical evaporative losses over a 3-day period were 1.0-2.0 mL.

Jar lids were required to prevent rapid drying of the soil samples, and thus CO_2 was quickly able to build up in the headspace of the jar to well above ambient CO_2 levels. Conversely, headspace O_2 concentrations may have become depleted due to limited air exchange (although this was not confirmed with measurements). To obtain gas flux measurements that were more representative of *in situ* conditions, headspaces needed to be purged with ambient air to remove CO_2 and provide O_2. However, we had observed that this rapid change in headspace conditions resulted in enhanced CO_2 fluxes immediately after purging, either due to a physical effect of built up CO_2 degassing from the soil water, or a rapid increase in microbial respiratory activity due to the sudden availability of O_2. Enhanced gas fluxes eventually decreased and returned to a relatively stable rate. Therefore, to obtain stable gas flux rates that are more representative of *in situ* conditions, jars were purged with air for 10 minutes and then left open for 1 hour prior to starting the gas flux measurement. After much trial of different purging and waiting times, this method resulted in the most consistent gas fluxes when measurements were repeated.

Gas flux measurements were performed using a 16-channel multiplexed infrared gas analyzer for CO_2 (LI-8100 and LI-8150, LI-COR Biosciences, Lincoln, Nebraska, USA). In brief, inlet and outlet tubing from the multiplexed system was connected to the soil sample jar lids forming a closed loop, and a pump circulated the headspace gas into the analyzing chamber. The

analyzer measured the accumulation of CO_2 in the headspace gas every second over an 8-minute period. Fluxes of CO_2 (F_{gas}, µmol kg^{-1} dry soil hr^{-1}) were calculated according to:

$$F_{gas} = \frac{PV}{RT}\frac{\Delta C_{gas}}{\Delta t}\frac{1}{m_{soil}}, \tag{3.4}$$

where P is the pressure (atm), V is the system volume (L, including the headspace, tubing and analyzing chamber volumes), R is the ideal gas constant (L atm K^{-1} mol^{-1}), T is the temperature (K), ΔC_{gas} is the change in gas mole fraction (µmol mol^{-1}), Δt is the time duration of the measurement (hr) and m_{soil} is the dry mass of soil (kg).

3.3.2 Preliminary results and discussion

Soil moisture content was expressed as either gravimetric soil moisture (g g^{-1} dry soil, hereafter, g g^{-1}) or percentage water-filled pore space (WFPS). To calculate % WFPS, we assumed that the highest moisture content samples were 100% saturated (after much trial and error of techniques for saturating the soil), and the porosity was calculated using the amount of water added to saturate the soil plus the residual moisture. In the case of Texture 1, the volume added for the second highest moisture content was used instead, since it appeared to be saturated and the highest moisture content appeared oversaturated. The % WFPS for each sample was then estimated as the total water volume (gravimetric moisture content × soil dry weight) divided by the total pore volume (porosity × soil volume). By this method of estimating porosity, the average porosity was 0.33, 0.35, and 0.40 for textures 1, 2 and 3, respectively, which are similar to reference values reported for these soil texture classes (Clapp and Hornberger, 1978). These porosity values corresponded to bulk densities of 1.78, 1.73 and 1.58 g cm^{-3}, assuming a particle density of 2.65 g cm^{-3}. Since the porosity and bulk density varied slightly between soil textures, a measurement of the gravimetric soil moisture converts to a different % WFPS for each soil texture.

Measured CO_2 fluxes are shown in Figure 3-6 as the average of 3 replicates with error bars representing standard error. Since CO_2 fluxes were relatively stable throughout the incubation period, the measurements reported here are those from the final timepoint measurement (20 days after the incubation started). The highest average CO_2 fluxes were recorded for Texture 1 (199 μmol g^{-1} dry soil hr^{-1}), and the maximum CO_2 fluxes recorded for Texture 2 and Texture 3 were similar (146 and 148 μmol g^{-1} dry soil hr^{-1}, respectively). The maximum CO_2 flux for Texture 1 occurred at a soil moisture of 0.187 g g^{-1}, for Texture 2 at 0.162 g g^{-1}, and for Texture 3 at 0.198 g g^{-1}, corresponding to % WFPS of 74%, 59%, and 57%, respectively. The fact that the overall magnitude of CO_2 fluxes in this experiment did not vary greatly between the soil textures is consistent with previous studies suggesting that kaolinite does not have a significant stabilizing effect on soil OM.

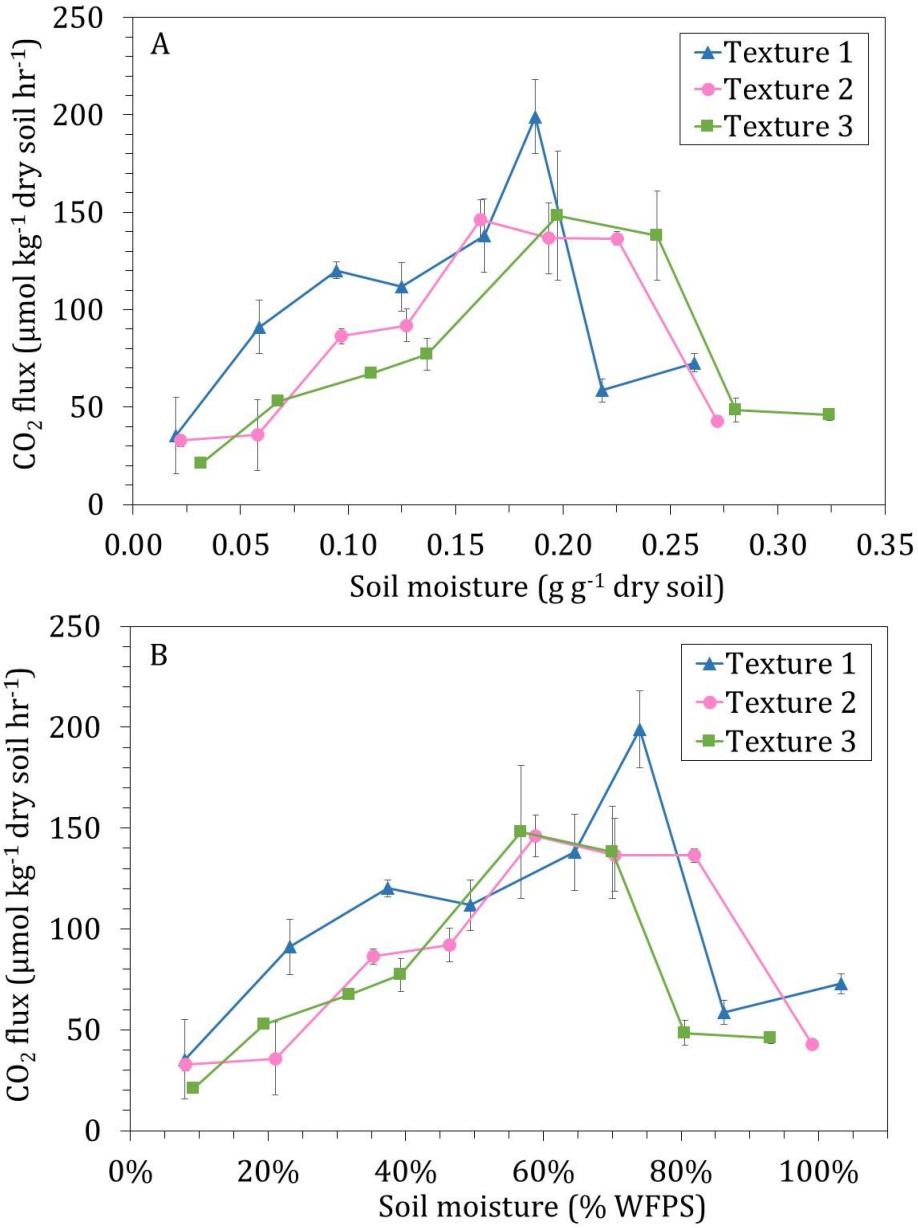

Figure 3-6: Measured CO_2 fluxes for soil types of increasing silt+clay content (Texture 1<Texture 2<Texture 3) at different soil moistures expressed gravimetrically (A) and on the basis of % WFPS (B) at the end of the incubation period. Error bars represent standard error (n=3). The value of % WFPS that falls above 100% for Texture 1 is due to the soil samples being slightly oversaturated with a shallow layer of overlying water.

For all soil textures, the general trend in CO_2 fluxes with moisture content was as expected, with the maximum fluxes occurring at moderate soil moisture and fluxes decreasing toward either moisture content extreme. These results were also consistent with the findings in Chapter 2 that CO_2 fluxes were non-zero under saturated conditions. Between the 3 soil textures, some differences started to emerge when CO_2 fluxes were plotted against gravimetric soil moisture. Though it is difficult to discern the exact soil moisture where the peak in CO_2 fluxes would occur without fitting a model to the data, the curves appeared slightly shifted relative to one another, with Texture 1 further to the left (toward lower soil moisture) and Texture 3 further to the right (toward higher soil moisture). This was consistent with the predictions of some empirical and more process-based models suggesting that the curve shifts to the right with increasing clay content in soil (Moyano *et al.*, 2012; Moyano *et al.*, 2013).

When soil moisture was expressed as % WFPS, however, the differences between curves appeared less obvious. This was explained by the difference in porosity between the 3 soil textures. When expressed gravimetrically, the soil moisture did not consider that soils of greater clay content tend to have greater porosity. Although soils were compacted slightly at the beginning of the experiment to keep the soil bulk density as similar as possible between all soil samples, there were still some unavoidable differences in soil volume, bulk density and thus, porosity between soil textures. By expressing soil moisture as % WFPS, we could essentially standardize for differences in soil porosity. This observation was also made by Moyano *et al.* (2013) in their model, which predicted large differences in relative microbial respiration among soils of varying porosity, but these differences were minimized by expressing soil moisture as relative water saturation instead of volumetric water content (Figure 3-7). Representing soil moisture as

% WFPS was also recommended by Scott *et al.*, (1996) as a way to combine the soil moisture and porosity parameters which could better account for the effects of soil texture and moisture.

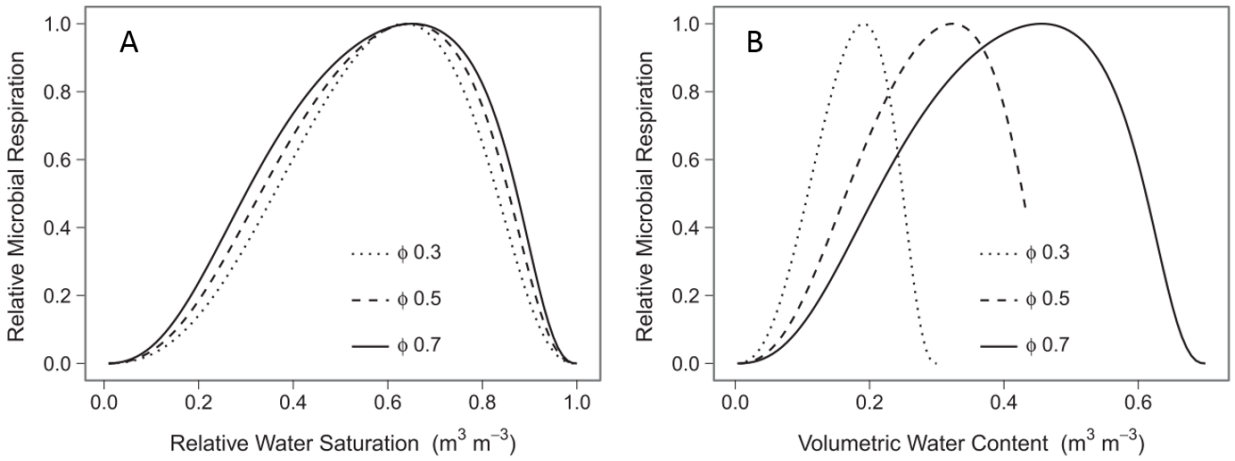

Figure 3-7: Figures obtained from Moyano *et al.* (2013) showing their model predictions for the relationship between relative respiration rate and soil moisture, expressed as either relative saturation (A) or volumetric water content (B).

Some differences remained between the 3 soil textures even when expressed as % WFPS. For example, Texture 1 appeared to have higher fluxes at low soil moisture compared to the other soil textures, which was also true for some of the model predictions when expressed as relative saturation (Moyano *et al.*, 2013; Ghezzehei *et al.*, 2019; Tang and Riley, 2019) Additionally, Texture 3 appeared to have lower fluxes at high soil moisture. One explanation for why Texture 3, which had the highest proportion of clay, had lower fluxes at high moisture content than the other soil textures is that the volume of anoxic microsites may increase with clay content, limiting aerobic respiration (Keiluweit *et al.*, 2018), although existing models do not account for this. The curve for Texture 3 appeared to be slightly narrower in shape, which is in agreement with a previous empirical model study (Moyano *et al.*, 2012) and other model predictions. However, definitive statements about each soil texture's relationship with soil moisture (as % WFPS) are difficult to make from this data since the error introduced by estimating the soil's effective porosity

in this case is largely unknown. A significant challenge faced by this study was the difficulty in standardizing relative saturation across soil textures due to their differing properties and the error in estimating porosity and bulk density. Regardless, it was clear from these results that the way in which soil moisture is expressed can change how we observe differences between soil textures.

3.3.3 Conclusion

This experimental design was a unique and novel method to look at a rarely tested hypothesis: that the relationship between soil CO_2 fluxes and soil moisture depends on the soil texture. Despite challenges with soil moisture adjustment and the estimation of % WFPS, these experimental results were useful to compare with predictions of existing models for the effect of soil texture on the CO_2 flux – soil moisture relationship. Although developing a mechanistic model that accounts for differences in soil texture was outside the scope of this thesis, previous studies have started building the theoretical framework that may advance the modelling of this effect. Therefore, in this chapter, I presented a review of these existing models and some preliminary work where an experimental design was developed to assess soil texture and soil moisture effects in a factorial batch experiment. Although improvements to the experimental methods are needed for future work, recognizing the need for more direct experimental evidence for the development of mechanistic models was an important step in improving our process-based understanding of soil CO_2 fluxes.

4 Conclusions and future research

4.1 Summary of key findings

The overall objective of this thesis was to advance the process-based understanding of how soil moisture and O_2 control soil CO_2 fluxes. Specifically, in Chapter 2, I aimed to validate the previous assumption that soil CO_2 fluxes are highest at moderate soil moisture due to the minimization of the combined limitations of both soil moisture and O_2. In this project, I performed a factorial batch experiment where the separate effects of soil moisture and O_2 were evaluated. Additionally, I aimed to demonstrate the contribution of anaerobic production of CO_2 to overall soil CO_2 emissions and develop a model that incorporates anaerobic processes as a source of CO_2.

In Chapter 2, the experimental results showed that CO_2 fluxes were maximal at moderate soil moisture in the oxic headspace incubations, as expected. However, CO_2 fluxes were maximal at the highest moisture content under the anoxic headspace incubations, where O_2 was consistently absent and its availability was therefore not changing with moisture content. These experimental data supported the assumption that O_2 limitation is the dominant factor that limits CO_2 fluxes at high soil moisture. Additionally, the influence of moisture content on CO_2 fluxes in the complete absence of O_2 demonstrated the independent effect of soil moisture on CO_2 fluxes due to either substrate diffusion limitations or physiological limitations, or a combination of both.

Our results demonstrated that previous models describing the effect of soil moisture on CO_2 fluxes underestimate fluxes at high soil moisture. Since previous models only considered aerobic respiration, they predicted the complete inhibition of CO_2 production under the O_2-limited conditions when soil is saturated with water. The previous approaches ignored the contribution of anaerobic processes to soil CO_2 production. Instead of the complete inhibition of CO_2 production, I measured substantial CO_2 fluxes from the saturated soil, though it was still reduced compared to

the moderately-saturated soil. In addition, I measured CO_2 fluxes from soil incubated under a completely O_2-free headspace, demonstrating the importance of considering anaerobic CO_2 production.

Results of the soil water chemistry analysis in Chapter 2 provided evidence for the types of anaerobic processes that were contributing to the measured CO_2 fluxes. Low molecular weight organic acids accumulated in the soil under the anoxic headspace incubations, likely as products of fermentation, which is an important step in anaerobic soil OM decomposition. The depletion of EAs under anoxic headspace incubations indicated that anaerobic respiration reactions had occurred. Additionally, the measured fluxes of CH_4 under anoxic headspace incubations indicated that, following a lag-time due to EA depletion, methanogenesis occurred which produced both CH_4 and CO_2. The absence of CH_4 fluxes from soils incubated under oxic headspace conditions indicated that either CH_4 was oxidized in oxic upper layers of the soil, or that soil conditions were not yet permissive of methanogenesis due to the presence of EAs.

The model developed in Chapter 2 was one of this project's novel contributions to the field of soil OM dynamics and CO_2 flux modelling. This model improved on previous models by considering the sum of both aerobic and anaerobic production of CO_2 from soil. As this is, to our knowledge, the first time an anaerobic component has been included in this type of model for the effect of soil moisture on CO_2 fluxes, we chose a relatively simple approach that could easily be incorporated into other existing models. The model developed in Chapter 2 used a version of the DAMM model of Davidson *et al.* (2012) to represent the aerobic respiration component, and a simple "lumped" term for the anaerobic production of CO_2 from soil. The incorporation of anaerobic sources of CO_2 into this type of model for the effect of soil moisture on CO_2 fluxes was

an important step in improving our ability to predict CO_2 fluxes across a range of soil moisture contents.

In addition to modelling CO_2 fluxes as a function of moisture content, it will also be critical to predict CO_2 fluxes across a range of different types of soil. One property that can vary between soil types that could affect CO_2 fluxes is soil texture. In Chapter 3, I reviewed the existing knowledge on the effect of soil texture on soil OM decomposition, and existing models that have started to provide a framework for investigating this predicted effect. While the effect of clay content on soil OM protection has been studied extensively in the past, very few studies have investigated the interactive effect between soil texture and soil moisture. The studies reviewed in Chapter 3 suggested that differences in soil texture may contribute to variation observed in the relationship between CO_2 fluxes and soil moisture. Reviewed models demonstrated the use of established empirical relationships and process-based understanding to make predictions about the effect of soil texture on CO_2 fluxes.

The factorial batch experiment conducted in Chapter 3 was a novel investigation into the effects of soil texture and soil moisture on CO_2 fluxes and their interactions. While challenges in the experimental methods made it difficult to make conclusive interpretations of the relationships, the experiment was a first step in comparing past model predictions with direct experimental data. The data agreed with some model predictions in that, when expressed on a gravimetric basis, the data was slightly shifted towards higher soil moisture for the soil with higher clay content. The results also agreed with past observations that relative saturation (% WFPS) was a useful representation of soil moisture since it accounts for differences in the porosity between soil textures. One important conclusion from Chapter 3 was that it is important to consider the way in

which soil moisture is expressed, what it represents in the context of the soil environment, and how this relates to the soil processes under study.

4.2 Recommendations for future research

The model developed in Chapter 2 was a first step to accurately representing soil CO_2 fluxes sourced from both aerobic and anaerobic soil processes. The simple representation of anaerobic sources as a single term for all anaerobic CO_2 production was useful in demonstrating the importance of considering anaerobic production in addition to aerobic respiration. This improvement could easily be incorporated into existing models that have already developed a framework to represent the effects of soil moisture on solute and gas diffusion and microbial physiological limitations (Ghezzehei *et al.*, 2019; Tang and Riley, 2019). The same mechanistic understanding of how soil moisture and O_2 affect microbial aerobic respiration could similarly be applied to anaerobic microbial processes. However, to improve our predictions of microbial reaction rates at the bulk soil scale, we will first need to improve our understanding of how conditions at the pore scale are affected by moisture content, as this represents the conditions experienced by the microbial community (Keiluweit *et al.*, 2017).

To go beyond the "lumped" term included in this model, future models could include predictions of individual microbial processes (*e.g.*, denitrification, acetoclastic methanogenesis), and could therefore also be expanded to include predictions of other products of microbial activity, such as N_2O and CH_4. To improve our ability to predict rates of different microbial metabolisms, there is a need for further experimental data that quantifies these processes. To better quantify the contributions of different metabolisms, it would be useful to collect time series data for cumulative CO_2 and CH_4, as well as the accumulation and depletion of other products and reactants. This could be collected by conducting a sacrificial batch experiment using a closed system where the

same measurements are repeated at different timepoints by destructively sampling replicates. While closed incubation experiments have their own limitations (*e.g.,* less representative of *in situ* conditions where gas products can diffuse away), they can facilitate accurate quantification of the mass balance.

The review of the effects of soil texture and soil moisture on CO_2 fluxes in Chapter 3 identified the lack of experimental studies investigating these two factors. The review of the existing models, however, identified that much work has been performed to conceptualize and start making model predictions about the possible interaction between soil texture and soil moisture. The experiment presented in Chapter 3 demonstrated the challenges in attempting to control both soil texture and soil moisture in a factorial batch experiment. Continued improvements to these experimental methods and additional factorial experiments will therefore be needed to better understand the mechanisms by which these two factors can interact. The continued development of models for CO_2 fluxes will rely on direct experimental evidence to incorporate process-based understanding of how soil texture can affect the relationship between CO_2 fluxes and soil moisture.

References

Alberts, B., A. Johnson, J. Lewis, M. Raff, K. Roberts, and P. Walter. 2008. *Molecular Biology of the Cell* (5th ed.). New York: Garland Science.

Amato, M., and J. N. Ladd. 1992. Decomposition of ^{14}C-labelled glucose and legume material in soils: properties influencing the accumulation of organic residue C and microbial biomass C. *Soil Biology and Biochemistry*, *24*(5), 445–464.

Arthur, E., P. Moldrup, P. Schjønning, and L. W. de Jonge. 2012. Linking particle size and pore size distribution parameters to soil gas transport properties. *Soil Science Society of America Journal*, *76*, 18–27.

Barré, P., O. Fernandez-Ugalde, I. Virto, B. Velde, and C. Chenu. 2014. Impact of phyllosilicate mineralogy on organic carbon stabilization in soils: Incomplete knowledge and exciting prospects. *Geoderma*, *235–236*, 382–395.

Bengtson, P., J. Barker, and S. J. Grayston. 2012. Evidence of a strong coupling between root exudation, C and N availability, and stimulated SOM decomposition caused by rhizosphere priming effects. *Ecology and Evolution*, *2*(8), 1843–1852.

Bengtson, P., and G. Bengtsson. 2007. Rapid turnover of DOC in temperate forests accounts for increased CO_2 production at elevated temperatures. *Ecology Letters*, *10*(9), 783–790.

Berner, E. K., and R. A. Berner. 2012. *Global Environment: Water, Air, and Geochemical Cycles* (2nd ed.). Princeton, NJ: Princeton University Press.

Bosatta, E., and G. I. Ågren. 1999. Soil organic matter quality interpreted thermodynamically. *Soil Biology and Biochemistry*, *31*(13), 1889–1891.

Boucher, O., P. Friedlingstein, B. Collins, and K. P. Shine. 2009. The indirect global warming potential and global temperature change potential due to methane oxidation. *Environmental Research Letters*, *4*(4), 044007.

Brewer, P. E., F. Calderón, M. Vigil, and J. C. von Fischer. 2018. Impacts of moisture, soil respiration, and agricultural practices on methanogenesis in upland soils as measured with stable isotope pool dilution. *Soil Biology and Biochemistry*, *127*, 239–251.

Burke, I. C., C. M. Yonker, W. J. Parton, C. V. Cole, K. Flach, and D. S. Schimel. 1989. Texture, climate, and cultivation effects on soil organic matter content in U.S. grassland soils. *Soil Science Society of America Journal*, *53*, 800–805.

Bush, E., and D. S. Lemmen. 2019. *Canada's Changing Climate Report*.

Chang, C. T., S. Sabaté, D. Sperlich, S. Poblador, F. Sabater, and C. Gracia. 2014. Does soil moisture overrule temperature dependence of soil respiration in Mediterranean riparian forests? *Biogeosciences*, *11*(21), 6173–6185.

Chenu, C., and A. T. Plante. 2006. Clay-sized organo-mineral complexes in a cultivation chronosequence: Revisiting the concept of the "primary organo-mineral complex." *European Journal of Soil Science*, *57*(4), 596–607.

Clapp, R. B., and G. M. Hornberger. 1978. Empirical equations for some soil hydraulic properties. *Water Resources Research*, *14*(4), 601–604.

Coleman, K., D. S. Jenkinson, G. J. Crocker, P. R. Grace, J. Klír, M. Körschens, … D. D. Richter. 1997. Simulating trends in soil organic carbon in long-term experiments using RothC-26.3. *Geoderma*, *81*(1–2), 29–44.

Davidson, E. A., E. Belk, and R. D. Boone. 1998. Soil water content and temperature as independent or confounded factors controlling soil respiration in a temperate mixed hardwood forest. *Global Change Biology*, *4*(2), 217–227.

Davidson, E. A., and I. A. Janssens. 2006. Temperature sensitivity of soil carbon decomposition and feedbacks to climate change. *Nature*, *440*, 165–173.

Davidson, E. A., S. Samanta, S. S. Caramori, and K. Savage. 2012. The Dual Arrhenius and Michaelis-Menten kinetics model for decomposition of soil organic matter at hourly to seasonal time scales. *Global Change Biology*, *18*(1), 371–384.

Davidson, E. A., S. E. Trumbore, and R. Amundson. 2000. Soil warming and organic carbon content. *Nature*, *408*, 789–790.

Delgado-Baquerizo, M., F. T. Maestre, P. B. Reich, T. C. Jeffries, J. J. Gaitan, D. Encinar, … B. K. Singh. 2016. Microbial diversity drives multifunctionality in terrestrial ecosystems. *Nature Communications*, *7*, 1–8.

Deng, Z., X. Qiu, J. Liu, N. Madras, X. Wang, and H. Zhu. 2016. Trend in frequency of extreme precipitation events over Ontario from ensembles of multiple GCMs. *Climate Dynamics*, *46*(9–10), 2909–2921.

Donat, M. G., A. L. Lowry, L. V. Alexander, P. A. O'Gorman, and N. Maher. 2016. More extreme precipitation in the world's dry and wet regions. *Nature Climate Change*, *6*(5), 508–513.

Doran, J. W. 2002. Soil health and global sustainability: Translating science into practice. *Agriculture, Ecosystems and Environment*, *88*(2), 119–127.

Dörr, H., L. Katruff, and I. Levin. 1993. Soil texture parameterization of the methane uptake in aerated soils. *Chemosphere*, *26*, 697–713.

Easterling, D. R. 2000. Climate extremes: Observations, modeling, and impacts. *Science*, *289*(5487), 2068–2074.

Ebrahimi, A., and D. Or. 2016. Microbial community dynamics in soil aggregates shape biogeochemical gas fluxes from soil profiles - upscaling an aggregate biophysical model. *Global Change Biology*, *22*(9), 3141–3156.

Ehrl, B. N., M. Gharasoo, and M. Elsner. 2018. Isotope fractionation pinpoints membrane permeability as a barrier to atrazine biodegradation in Gram-negative Polaromonas sp. Nea-C. *Environmental Science and Technology*, *52*(7), 4137–4144. research-article.

Eswaran, H., E. Berg, and P. Reich. 1993. Organic carbon in soils of the world. *Soil Sci Soc Am J*, *57*, 192–194.

Foley, J. A., R. DeFries, G. P. Asner, C. Barford, G. Bonan, S. R. Carpenter, … P. K. Snyder. 2005. Global consequences of land use. *Science*, *309*, 570–574.

Forster, P., V. Ramaswamy, P. Artaxo, T. Berntsen, R. Betts, D. W. Fahey, … R. Van Dorland. 2007. Changes in Atmospheric Constituents and in Radiative Forcing. In S. Solomon, D. Qin, M. Manning, Z. Chen, M. Marquis, K. B. Averyt, … H. L. Miller (Eds.), *Climate Change 2007: The Physical Science Basis. Contribution of Working Group I to the Fourth Assessment Report of the Intergovernmental Panel on Climate Change.* Cambridge, United Kingdom and New York, NY, USA.

Freeman, C., N. Ostle, and H. Kang. 2001. An enzymic "latch" on a global carbon store. *Nature*, *409*(6817), 149–149.

Fritsch, F., and R. Carlson. 1980. Monotone piecewise cubic interpolation. *SIAM Journal on Numerical Analysis*, *7*(2), 238–246.

Froelich, P. N., G. P. Klinkhammer, M. L. Bender, N. A. Luedtke, G. R. Heath, D. Cullen, … V. Maynard. 1979. Early oxidation of organic matter in pelagic sediments of the eastern equatorial Atlantic: suboxic diagenesis. *Geochimica et Cosmochimica Acta*, *43*(7), 1075–1090.

Fujikawa, T., and T. Miyazaki. 2005. Effects of bulk density and soil type on the gas diffusion coefficient in repacked and undisturbed soils. *Soil Science*, *170*(11), 892–901.

Gao, C., M. Sander, S. Agethen, and K. H. Knorr. 2019. Electron accepting capacity of dissolved and particulate organic matter control CO2 and CH4 formation in peat soils. *Geochimica et Cosmochimica Acta*, *245*, 266–277.

Gardner, W. H. 1986. Water Content. In A. Kiute (Ed.), *Methods of Soil Analysis: Physical and Mineralogical Methods, Agronomy Series 9 (Part 1).* (pp. 493–544). Madison, Wisconsin: Soil Science Society of America.

Gee, G. W., and J. W. Bauder. 1986. Particle Size Analysis. In A. Klute (Ed.), *Methods of Soil Analysis: Part 1. Physical and Mineralogical Methods* (pp. 383–411). Madison, USA.: Soil Science Society of America.

Gharasoo, M., M. Thullner, and M. Elsner. 2017. Introduction of a new platform for parameter estimation of kinetically complex environmental systems. *Environmental Modelling and Software*, *98*, 12–20.

Ghezzehei, T. A., B. Sulman, C. L. Arnold, N. A. Bogie, and A. A. Berhe. 2019. On the role of soil water retention characteristic on aerobic microbial respiration. *Biogeosciences*, *16*, 1187–1209.

Giardina, C. P., and M. G. Ryan. 2000. Evidence that decomposition rates of organic carbon in mineral soil do not vary with temperature. *Nature*, *404*(6780), 858–861.

Gregorich, E. G., R. P. Voroney, and R. G. Kachanoski. 1991. Turnover of carbon through the microbial biomass in soils with different texture. *Soil Biology and Biochemistry*, *23*(8), 799–805.

Hack, N., C. Reinwand, G. Abbt-Braun, H. Horn, and F. H. Frimmel. 2015. Biodegradation of

phenol, salicylic acid, benzenesulfonic acid, and iomeprol by *Pseudomonas fluorescens* in the capillary fringe. *Journal of Contaminant Hydrology*, *183*, 40–54.

Hall, S. J., J. Treffkorn, and W. L. Silver. 2014. Breaking the enzymatic latch: impacts of reducing conditions on hydrolytic enzyme activity in tropical forest soils. *Ecology*, *95*(10), 2964–2973.

Halverson, L. J., T. M. Jones, and M. K. Firestone. 2000. Release of intracellular solutes by four soil bacteria exposed to dilution stress. *Soil Science Society of America Journal*, *64*(5), 1630–1637.

Harper, C. W., J. M. Blair, P. A. Fay, A. K. Knapp, and J. D. Carlisle. 2005. Increased rainfall variability and reduced rainfall amount decreases soil CO_2 flux in a grassland ecosystem. *Global Change Biology*, *11*(2), 322–334.

Hartley, I. P., D. W. Hopkins, M. H. Garnett, M. Sommerkorn, and P. A. Wookey. 2008. Soil microbial respiration in arctic soil does not acclimate to temperature. *Ecology Letters*, *11*(10), 1092–1100.

Hartley, I. P., D. W. Hopkins, M. Sommerkorn, and P. A. Wookey. 2010. The response of organic matter mineralisation to nutrient and substrate additions in sub-arctic soils. *Soil Biology and Biochemistry*, *42*(1), 92–100.

Hassink, J. 1997. The capacity of soils to preserve organic C and N by their association with clay and silt particles. *Plant and Soil*, *191*, 77–87.

Herndon, E. M., B. F. Mann, T. Roy Chowdhury, Z. Yang, S. D. Wullschleger, D. Graham, … B. Gu. 2015. Pathways of anaerobic organic matter decomposition in tundra soils from Barrow, Alaska. *Journal of Geophysical Research G: Biogeosciences*, *120*(11), 2345–2359.

IPCC. 2018. *Global warming of 1.5°C. An IPCC Special Report on the impacts of global warming of 1.5°C above pre-industrial levels and related global greenhouse gas emission pathways, in the context of strenthening the global respones to the threat of climate change,*. (V. Masson-Delmotte, P. Zhai, H. O. Pörtner, D. Roberts, J. Skea, P. R. Shukla, … T. W. T. Maycock, M. Tignor, Eds.).

IPCC. 2019. *Climate change and land. An IPCC Special Report on climate change, desertification, land degradation, sustainable land management, food security, and greenhouse gas fluxes in terrestrial ecosystems*.

Jagadamma, S., M. A. Mayes, J. M. Steinweg, and S. M. Schaeffer. 2014. Substrate quality alters the microbial mineralization of added substrate and soil organic carbon. *Biogeosciences*, *11*(17), 4665–4678.

Jenkinson, D. S., and J. M. Oades. 1979. A method for measuring adenosine triphosphate in soil. *Soil Biology and Biochemistry*, *11*(2), 193–199.

Joergensen, R. G. 1996. The fumigation-extraction method to estimate soil microbial biomass: Calibration of the k_{EC} value. *Soil Biology & Biochemistry*, *28*(1), 25–31.

Keiluweit, M., K. Gee, A. Denney, and S. Fendorf. 2018. Anoxic microsites in upland soils dominantly controlled by clay content. *Soil Biology and Biochemistry*, *118*, 42–50.

Keiluweit, M., T. Wanzek, M. Kleber, P. Nico, and S. Fendorf. 2017. Anaerobic microsites have an unaccounted role in soil carbon stabilization. *Nature Communications*, *8*(1), 1–8.

Killham, K. 1985. A physiological determination of the impact of environmental stress on the activity of microbial biomass. *Environmental Pollution. Series A, Ecological and Biological*, *38*(3), 283–294.

Knorr, K. H., and C. Blodau. 2009. Impact of experimental drought and rewetting on redox transformations and methanogenesis in mesocosms of a northern fen soil. *Soil Biology and Biochemistry*, *41*(6), 1187–1198.

Knorr, K. H., G. Lischeid, and C. Blodau. 2009. Dynamics of redox processes in a minerotrophic fen exposed to a water table manipulation. *Geoderma*, *153*(3–4), 379–392.

Kunc, F., and G. Stotzky. 1974. Effect of clay minerals on heterotrophic microbial activity in soil. *Soil Science*, *118*, 189–195.

Lal, R. 2004. Soil carbon sequestration impacts on global climate change and food security. *American Association for the Advancement of Science*, *304*(5677), 1623–1627.

Lal, R. 2010. Managing soils and ecosystems for mitigating anthropogenic carbon emissions and advancing global food security. *BioScience*, *60*(9), 708–721.

LaRowe, D. E., and J. P. Amend. 2019. The energetics of fermentation in natural settings. *Geomicrobiology Journal*, *36*(6), 492–505.

LaRowe, D. E., and P. Van Cappellen. 2011. Degradation of natural organic matter: A thermodynamic analysis. *Geochimica et Cosmochimica Acta*, *75*(8), 2030–2042.

Lawrence, D. M., C. D. Koven, S. C. Swenson, W. J. Riley, and A. G. Slater. 2015. Permafrost thaw and resulting soil moisture changes regulate projected high-latitude CO_2 and CH_4 emissions. *Environmental Research Letters*, *10*(9).

Le Quéré, C., M. R. Raupach, J. G. Canadell, G. Marland, L. Bopp, P. Ciais, … F. I. Woodward. 2009. Trends in the sources and sinks of carbon dioxide. *Nature Geoscience*, *2*(12), 831–836.

Lellei-Kovács, E., E. Kovács-Láng, Z. Botta-Dukát, T. Kalapos, B. Emmett, and C. Beier. 2011. Thresholds and interactive effects of soil moisture on the temperature response of soil respiration. *European Journal of Soil Biology*, *47*(4), 247–255.

Linn, D. M., and J. W. Doran. 1984. Effect of water-filled pore space on carbon dioxide and nitrous oxide production in tilled and nontilled soils. *Soil Science Society of America Journal*, *48*(6), 1267–1272.

Lloyd, J., and J. A. Taylor. 1994. On the temperature dependence of soil respiration. *Functional Ecology*, *8*(3), 315–323.

Lovley, D. R., J. D. Coates, E. L. Blunt-Harris, E. J. P. Phillips, and J. C. Woodward. 1996. Humic substances as electron acceptors for microbial respiration. *Nature*, *382*, 445–448.

Lützow, M. V., I. Kögel-Knabner, K. Ekschmitt, E. Matzner, G. Guggenberger, B. Marschner, and H. Flessa. 2006. Stabilization of organic matter in temperate soils: Mechanisms and

their relevance under different soil conditions - A review. *European Journal of Soil Science*, *57*(4), 426–445.

Lynd, L. R., P. J. Weimer, W. H. van Zyl, and I. S. Pretorius. 2002. Microbial celullose utilizaton: Fundamentals and biotechnology. *Bioresource Technology*, *66*(3), 506–577.

Makarov, M. I., M. S. Shuleva, T. I. Malysheva, and O. V. Menyailo. 2013. Solubility of the labile forms of soil carbon and nitrogen in K_2SO_4 of different concentrations. *Eurasian Soil Science*, *46*(4), 369–374.

Manzoni, S., J. P. Schimel, and A. Porporato. 2011. Responses of soil microbial communities to water stress: results from a meta-analysis. *Ecology*, *93*(4), 930–938.

Marozava, S., A. H. Meyer, A. Perez-de-Mora, M. Gharasoo, L. Zhuo, H. Wang, … M. Elsner. 2019. Mass transfer limitation during slow anaerobic biodegradation of 2-methylnaphthalene. *Environmental Science & Technology*, *53*(16), 9481–9490.

McNicol, G., and W. L. Silver. 2014. Separate effects of flooding and anaerobiosis on soil greenhouse gas emissions and redox sensitive biogeochemistry. *Journal of Geophysical Research: Biogeosciences*, *119*, 557–566.

Megonigal, J. P., M. E. Mines, and P. T. Visscher. 2004. Anaerobic metabolism: Linkages to trace gases and aerobic processes. In W. H. Schlesinger (Ed.), *Biogeochemistry* (pp. 350–362). Oxford, UK: Elsevier-Pergamon.

Moldrup, P., T. Olesen, T. Komatsu, P. Schjønning, and D. E. Rolston. 2001. Tortuosity, diffusivity, and permeability in the soil liquid and gaseous phases. *Soil Science Society of America Journal*, *65*, 613–623.

Moldrup, P., T. Olesen, P. Schjønning, T. Yamaguchi, and D. E. Rolston. 2000. Predicting the gas diffusion coefficient in undisturbed soil from soil water characteristics. *Soil Science Society of America Journal*, *64*, 94–100.

Moore, T. R., and M. Dalva. 1997. Methane and carbon dioxide exchange potentials of peat soils in aerobic and anaerobic laboratory incubations. *Soil Biology and Biochemistry*, *29*(8), 1157–1164.

Moyano, F. E., S. Manzoni, and C. Chenu. 2013. Responses of soil heterotrophic respiration to moisture availability: An exploration of processes and models. *Soil Biology and Biochemistry*, *59*, 72–85.

Moyano, F. E., N. Vasilyeva, L. Bouckaert, F. Cook, J. Craine, J. Curiel Yuste, … C. Chenu. 2012. The moisture response of soil heterotrophic respiration: interaction with soil properties. *Biogeosciences*, *9*, 1173–1182.

Moyano, F. E., N. Vasilyeva, and L. Menichetti. 2018. Diffusion based modelling of combined temperature and moisture effects on carbon fluxes of mineral soils. *Biogeosciences Discussions*, 5031–5045.

Natali, S. M., J. D. Watts, B. M. Rogers, S. Potter, S. M. Ludwig, A. Selbmann, … Y. Wang. 2019. Large loss of CO_2 in winter observed across the northern permafrost region. *Nature Climate Change*, *9*, 852–857.

Olesen, T., P. Moldrup, T. Yamaguchi, and D. E. Rolston. 2001. Constant slope impedance factor model for predicting the solute diffusion coefficient in unsaturated soil. *Soil Science, 166*(2), 89–96.

Or, D., B. F. Smets, J. M. Wraith, A. Dechesne, and S. P. Friedman. 2007. Physical constraints affecting bacterial habitats and activity in unsaturated porous media - a review. *Advances in Water Resources, 30*, 1505–1527.

Orchard, V. A., and F. J. Cook. 1983. Relationship between soil respiration and soil moisture. *Soil Biology and Biochemistry*, *15*(4), 447–453.

Pallud, C., Y. Masue-Slowey, and S. Fendorf. 2010. Aggregate-scale spatial heterogeneity in reductive transformation of ferrihydrite resulting from coupled biogeochemical and physical processes. *Geochimica et Cosmochimica Acta, 74*(10), 2811–2825.

Parkin, T. B. 1987. Soil microsites as a source of denitrification variability. *Soil Science Society of America Journal*, *51*, 1194–1199.

Parsons, C. T., R. M. Couture, E. O. Omoregie, F. Bardelli, J. M. Greneche, G. Roman-Ross, and L. Charlet. 2013. The impact of oscillating redox conditions: Arsenic immobilisation in contaminated calcareous floodplain soils. *Environmental Pollution, 178*, 254–263.

Parton, W. J., D. W. Anderson, C. V. Cole, and J. W. B. Steward. 1983. Simulation of soil organic matter formation and mineralization in semiarid agroecosystems. In R. R. Lowrance, R. L. Todd, L. E. Asmussen, & R. A. Leonard (Eds.), *Nutrient cycling in agricultural ecosystems*. Athens, Georgia: The Univ. of Georgia, Colledge of Agriculture Experiment Stations, Special Pub. No. 23.

Paustian, K., J. Six, E. T. Elliott, and H. W. Hunt. 2000. Management options for reducing CO_2 emissions from agricultural soils. *Biogeochemistry, 48*, 147–163.

Peters, G. P., R. M. Andrew, T. Boden, J. G. Canadell, P. Ciais, C. Le Quéré, … C. Wilson. 2013. The challenge to keep global warming below 2 °C. *Nature Climate Change*, *3*(1), 4–6.

Peters, G. P., G. Marland, C. Le Quéré, T. Boden, J. G. Canadell, and M. R. Raupach. 2012. Rapid growth in CO_2 emissions after the 2008-2009 global financial crisis. *Nature Climate Change, 2*(1), 2–4.

Plante, A. F., R. T. Conant, C. E. Stewart, K. Paustian, and J. Six. 2006. Impact of soil texture on the distribution of soil organic matter in physical and chemical fractions. *Soil Science Society of America Journal*, *70*(1), 287–296.

Poll, C., S. Marhan, F. Back, P. A. Niklaus, and E. Kandeler. 2013. Field-scale manipulation of soil temperature and precipitation change soil CO_2 flux in a temperate agricultural ecosystem. *Agriculture, Ecosystems and Environment*, *165*, 88–97.

Ponnamperuma, F. N. 1972. The Chemistry of Submerged Soils. *Advances in Agronomy*, *24*, 29–96.

Pronk, G. J., K. Heister, and I. Kögel-Knabner. 2013. Is turnover and development of organic matter controlled by mineral composition? *Soil Biology and Biochemistry*, *67*, 235–244.

Raich, J. W., and C. S. Potter. 1995. Global patterns of carbon-dioxide emissions from soils. *Global Biogeochemical Cycles*, *9*(1), 23–36.

Raich, J. W., E. B. Rastetter, J. M. Melillo, D. W. Kicklighter, P. A. Steudler, B. J. Peterson, … C. J. Vörösmarty. 1991. Potential net primary productivity in South America application of a global model. *Ecological Applications*, *1*(4), 399–429.

Raich, J. W., and W. H. Schlesinger. 1992. The global carbon dioxide flux in soil respiration and its relationship to vegetation and climate. *Tellus*, *44B*, 81–99.

Redmile-Gordon, M., R. P. White, and P. C. Brookes. 2011. Evaluation of substitutes for paraquat in soil microbial ATP determinations using the trichloroacetic acid based reagent of Jenkinson and Oades (1979). *Soil Biology and Biochemistry*, *43*(5), 1098–1100.

Rezanezhad, F., R.-M. Couture, R. Kovac, D. O'Connell, and P. Van Cappellen. 2014. Water table fluctuations and soil biogeochemistry: An experimental approach using an automated soil column system. *Journal of Hydrology*, *509*, 245–256.

Rezanezhad, F., J. S. Price, W. L. Quinton, B. Lennartz, T. Milojevic, and P. Van Cappellen. 2016. Structure of peat soils and implications for water storage, flow and solute transport: A review update for geochemists. *Chemical Geology*, *429*, 75–84.

Richardson, D., H. Felgate, N. Watmough, A. Thomson, and E. Baggs. 2009. Mitigating release of the potent greenhouse gas N_2O from the nitrogen cycle - could enzymic regulation hold the key? *Trends in Biotechnology*, *27*(7), 388–397.

Roy Chowdhury, T., E. M. Herndon, T. J. Phelps, D. A. Elias, B. Gu, L. Liang, … D. E. Graham. 2015. Stoichiometry and temperature sensitivity of methanogenesis and CO_2 production from saturated polygonal tundra in Barrow, Alaska. *Global Change Biology*, *21*(2), 722–737.

Saidy, A. R., R. J. Smernik, J. A. Baldock, K. Kaiser, J. Sanderman, and L. M. Macdonald. 2012. Effects of clay mineralogy and hydrous iron oxides on labile organic carbon stabilisation. *Geoderma*, *173–174*, 104–110.

Scharlemann, J. P. W., E. V. J. Tanner, R. Hiederer, and V. Kapos. 2014. Global soil carbon: Understanding and managing the largest terrestrial carbon pool. *Carbon Management*, *5*(1), 81–91.

Schimel, D. S. 1995. Terrestrial ecosystems and the carbon cycle. *Global Change Biology*, *1*, 77–91.

Schimel, J., T. C. Balser, and M. Wallenstein. 2007. Microbial stress-response physiology and its implications for ecosystem function. *Ecology*, *88*(6), 1386–1394.

Schimel, J. P. 2018. Life in dry soils: Effects of drought on soil microbial communities and processes. *Annual Review of Ecology, Evolution, and Systematics*, *49*, 409–432.

Schipper, L. A., J. K. Hobbs, S. Rutledge, and V. L. Arcus. 2014. Thermodynamic theory explains the temperature optima of soil microbial processes and high Q10 values at low temperatures. *Global Change Biology*, *20*(11), 3578–3586.

Schjønning, P., I. K. Thomsen, J. P. Møberg, H. De Jonge, K. Kristensen, and B. T. Christensen. 1999. Turnover of organic matter in differently textured soils I. Physical characteristics of structurally disturbed and intact soils. *Geoderma*, *89*(3–4), 177–198.

Schjønning, P., I. K. Thomsen, P. Moldrup, and B. T. Christensen. 2003. Linking soil microbial activity to water- and air-phase contents and diffusivities. *Soil Science Society of America Journal*, *67*(1), 156–165.

Schlesinger, W. H. 1977. Carbon balance in terrestrial detritus. *Annual Review of Ecology and Systematics*, *8*, 51–81.

Schlesinger, W. H., and E. S. Bernhardt. 2013. *Biogeochemistry: an analysis of global change* (3rd ed.). Waltham, Mass.: Academic Press.

Schuur, E. A., and P. A. Matson. 2001. Net primary productivity and nutrient cycling across a mesic to wet precipitation gradient in Hawaiian montane forest. *Oecologia*, *128*(3), 431–442.

Scott, N. A., C. V. Cole, E. T. Elliot, and S. A. Huffman. 1996. Soil textural control on decomposition and soil organic matter dynamics. *Soil Science Society of America Journal*, *60*, 1102–1109.

Segers, R. 1998. Methane production and methane consumption: a review of processes underlying wetland methane fluxes. *Biogeochemistry*, *41*, 23–51.

Sexstone, A. J., N. P. Revsbech, T. B. Parkin, and J. M. Tiedje. 1985. Direct measurement of oxygen profiles and denitrification rates in soil aggregates. *Soil Science Society of America Journal*, *49*, 645–651.

Sey, B. K., A. M. Manceur, J. K. Whalen, E. G. Gregorich, and P. Rochette. 2008. Small-scale heterogeneity in carbon dioxide, nitrous oxide and methane production from aggregates of a cultivated sandy-loam soil. *Soil Biology and Biochemistry*, *40*(9), 2468–2473.

Sierra, C. A., S. Malghani, and H. W. Loescher. 2017. Interactions among temperature, moisture, and oxygen concentrations in controlling decomposition rates in a boreal forest soil. *Biogeosciences*, *14*(3), 703–710.

Silver, W. L., A. E. Lugo, and M. Keller. 1999. Soil oxygen availability and biogeochemistry along rainfall and topographic gradients in upland wet tropical forest soils. *Biogeochemistry*, *44*, 301–328.

Singh, B. K., R. D. Bardgett, P. Smith, and D. S. Reay. 2010. Microorganisms and climate change: Terrestrial feedbacks and mitigation options. *Nature Reviews Microbiology*, *8*, 779–790.

Six, J., R. T. Conant, E. a Paul, and K. Paustian. 2002. Stabilization mechanisms of soil organic matter: Implications for C-saturation of soils. *Plant and Soil*, *241*, 155–176.

Skopp, J., M. D. Jawson, and J. W. Doran. 1990. Steady-state aerobic microbial activity as a function of soil water content. *Soil Science Society of America Journal*, *54*, 1619–1625.

Smith, P. 2004. Carbon sequestration in croplands: The potential in Europe and the global

context. *European Journal of Agronomy*, *20*(3), 229–236.

Smith, P., D. Martino, Z. Cai, D. Gwary, H. Janzen, P. Kumar, … J. Smith. 2008. Greenhouse gas mitigation in agriculture. *Philosophical Transactions of the Royal Society B: Biological Sciences*, *363*(1492), 789–813.

Sørensen, L. H. 1972. Stabilization of newly formed amino acid metabolites in soil by clay minerals. *Soil Science*, *114*(1), 5–11.

Sørensen, L. H. 1975. The influence of clay on the rate of decay of amino acid metabolites synthesized in soils during decomposition of cellulose. *Soil Biology and Biochemistry*, *7*(2), 171–177.

Strack, M., E. Kellner, and J. M. Waddington. 2005. Dynamics of biogenic gas bubbles in peat and their effects on peatland biogeochemistry. *Global Biogeochemical Cycles*, *19*(1), 1–9.

Sulman, B. N., R. P. Phillips, A. C. Oishi, E. Shevliakova, and S. W. Pacala. 2014. Microbe-driven turnover offsets mineral-mediated storage of soil carbon under elevated CO_2. *Nature Climate Change*, *4*(12), 1099–1102.

Tang, J., and W. J. Riley. 2019. A theory of effective microbial substrate affinity parameters in variably saturated soils and an example application to aerobic soil heterotrophic respiration. *Journal of Geophysical Research: Biogeosciences*.

Thomsen, I. K., P. Schjønning, and B. Jensen. 1999. Turnover of organic matter in differently texture soils II. Microbial activity as influenced by soil water regimes. *Geoderma*, *89*, 199–218.

Tokida, T., T. Miyazaki, M. Mizoguchi, and K. Seki. 2005. In situ accumulation of methane bubbles in a natural wetland soil. *European Journal of Soil Science*, *56*(3), 389–395.

Totsche, K. U., W. Amelung, M. H. Gerzabek, G. Guggenberger, E. Klumpp, C. Knief, … I. Kögel-Knabner. 2018. Microaggregates in soils. *Journal of Plant Nutrition and Soil Science*, *181*(1), 104–136.

Treves, D. S., B. Xia, J. Zhou, and J. M. Tiedje. 2003. A two-species test of the hypothesis that spatial isolation influences microbial diversity in soil. *Microbial Ecology*, *45*(1), 20–28.

Van Cappellen, P., and X. Wang. 1995. Metal cycling in surface sediments: Modeling the interplay of transport and reaction. In H. E. Allen (Ed.), *Metal Contaminated Aquatic Sediments* (p. 44). Chelsea, Mich: Ann Arbor Press.

Van Genuchten, M. 1980. A closed-form equation for predicting the hydraulic conductivity of unsaturated soils. *Soil Science Society of America Journal*, *44*(5), 892–898.

Vance, E. D., P. C. Brookes, and D. S. Jenkinson. 1987. An extraction method for measuring soil microbial biomass C. *Soil Biology and Biochemistry*, *19*(6), 703–707.

Wang, W. J., R. C. Dalal, P. W. Moody, and C. J. Smith. 2003. Relationships of soil respiration to microbial biomass, substrate availability and clay content. *Soil Biology and Biochemistry*, *35*(2), 273–284.

Wickland, K. P., and J. C. Neff. 2008. Decomposition of soil organic matter from boreal black

spruce forest: Environmental and chemical controls. *Biogeochemistry*, *87*(1), 29–47.

Wiesmeier, M., R. Hübner, P. Spörlein, U. Geuß, E. Hangen, A. Reischl, … I. Kögel-Knabner. 2014. Carbon sequestration potential of soils in southeast Germany derived from stable soil organic carbon saturation. *Global Change Biology*, *20*(2), 653–665.

Williams, M. D., and M. Oostrom. 2000. Oxygenation of anoxic water in a fluctuating water table system: An experimental and numerical study. *Journal of Hydrology*, *230*(1–2), 70–85.

Yan, Z., B. Bond-Lamberty, K. E. Todd-Brown, V. L. Bailey, S. Li, C. Liu, and C. Liu. 2018. A moisture function of soil heterotrophic respiration that incorporates microscale processes. *Nature Communications*, *9*, 2562.

Zhang, Y., and M. G. Schaap. 2017. Weighted recalibration of the Rosetta pedotransfer model with improved estimates of hydraulic parameter distributions and summary statistics (Rosetta3). *Journal of Hydrology*, *547*, 39–53.

Zheng, J., P. E. Thornton, S. L. Painter, B. Gu, S. D. Wullschleger, and D. E. Graham. 2019. Modeling anaerobic soil organic carbon decomposition in Arctic polygon tundra: Insights into soil geochemical influences on carbon mineralization. *Biogeosciences*, *16*(3), 663–680.

Zhuang, J., J. F. McCarthy, E. Perfect, L. M. Mayer, and J. D. Jastrow. 2008. Soil water hysteresis in water-stable microaggregates as affected by organic matter. *Soil Science Society of America Journal*, *72*(1), 212–220.

Appendix – Additional experimental results from Chapter 2

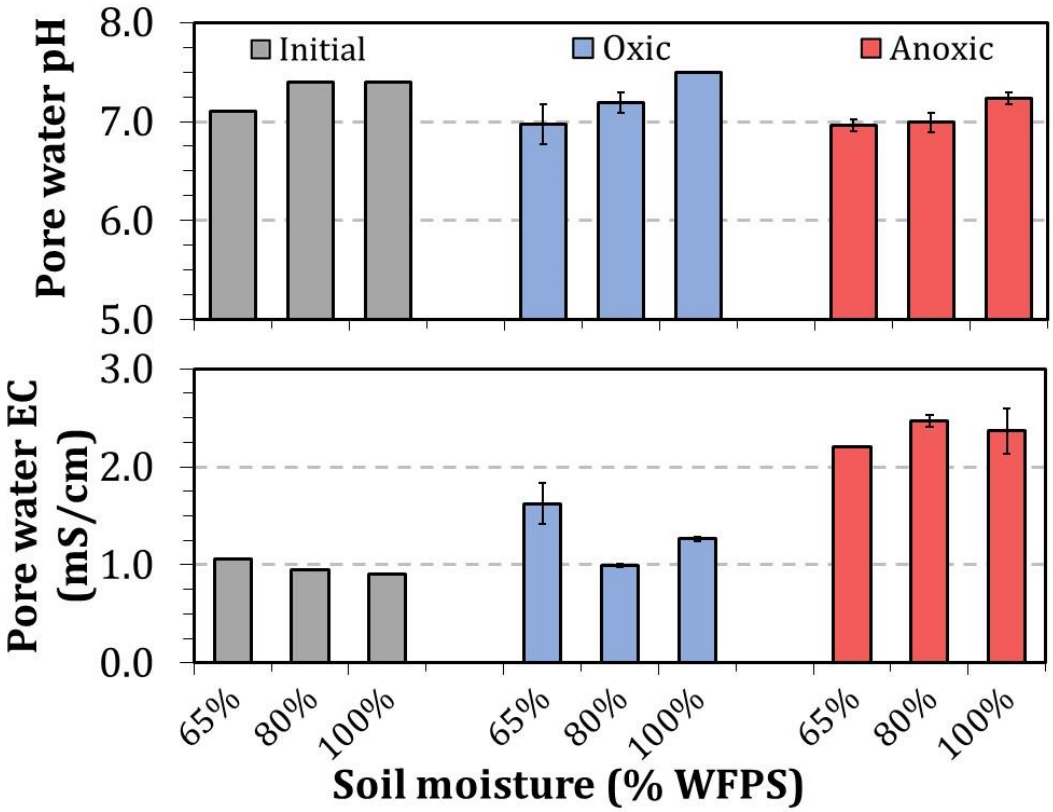

Figure A-1: Soil pore water pH (top) and electrical conductivity (EC; bottom) from direct pore water extractions in the Chapter 2 experiment. Measurements are from direct pore water extractions (see section *2.2.3*) at the beginning of the experiment (grey) and at the end (oxic – blue, anoxic – red). Error bars represent standard deviation (n=3), not shown for initial samples (n=1).

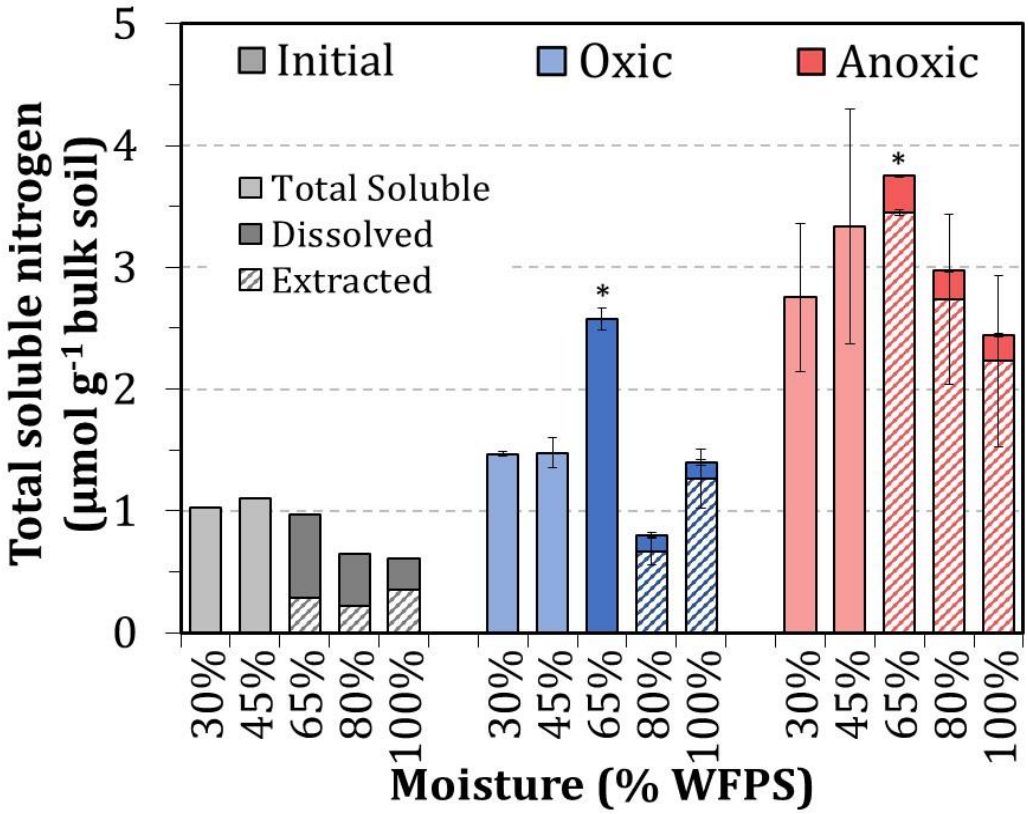

Figure A-2: Total soluble nitrogen in soil pore water and K_2SO_4 extracts measured at the beginning (initial – grey) and end (oxic – blue and anoxic – red) of the incubation in the Chapter 2 experiment. The concentrations measured in the K_2SO_4 extracts represent the total soluble concentration (lighter shade), the concentrations measured in the pore water represent the dissolved fraction of the soluble concentration (darker shade) and the difference between these concentrations represents the extracted fraction (striped). Extraction and analytical methods were described in section *2.2.3*. Error bars represent standard deviation (n=3, *n=2), not shown for initial samples (n=1).

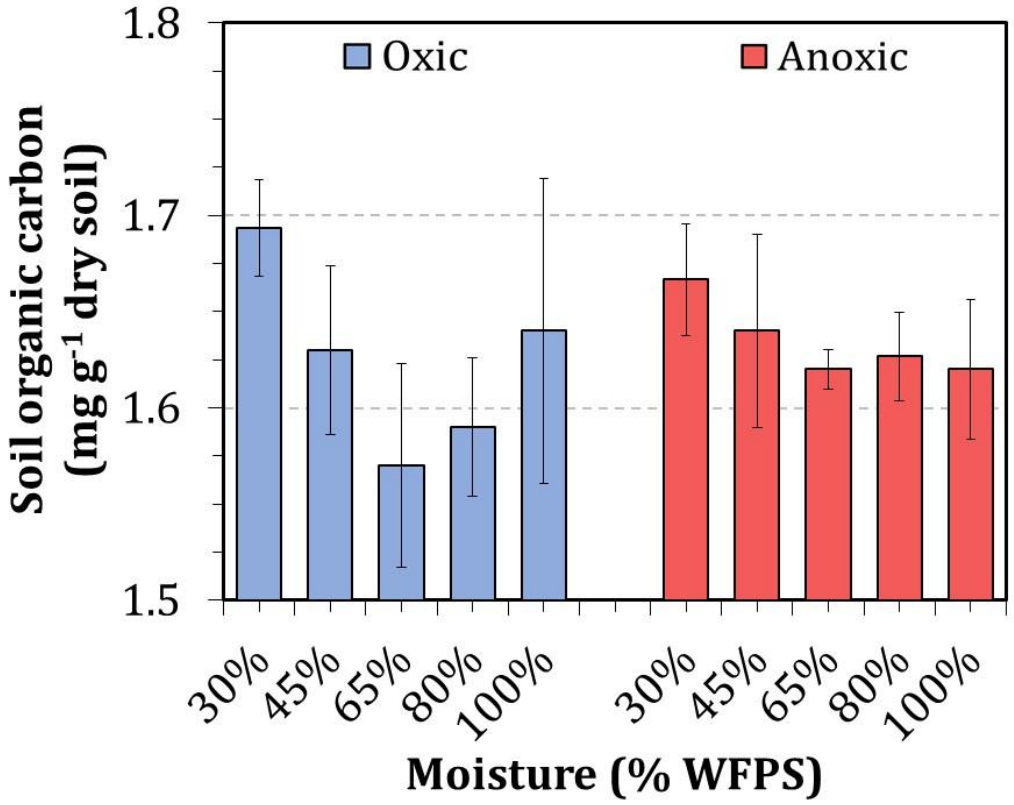

Figure A-3: Soil organic carbon measured for oxic (blue) and anoxically (red) incubated soil samples at the end of the incubation in the Chapter 2 experiment. Measurements were made using a CHNS Carbo Erba analyzer as described in section *2.2.1.* Error bars represent standard deviation (n=3).

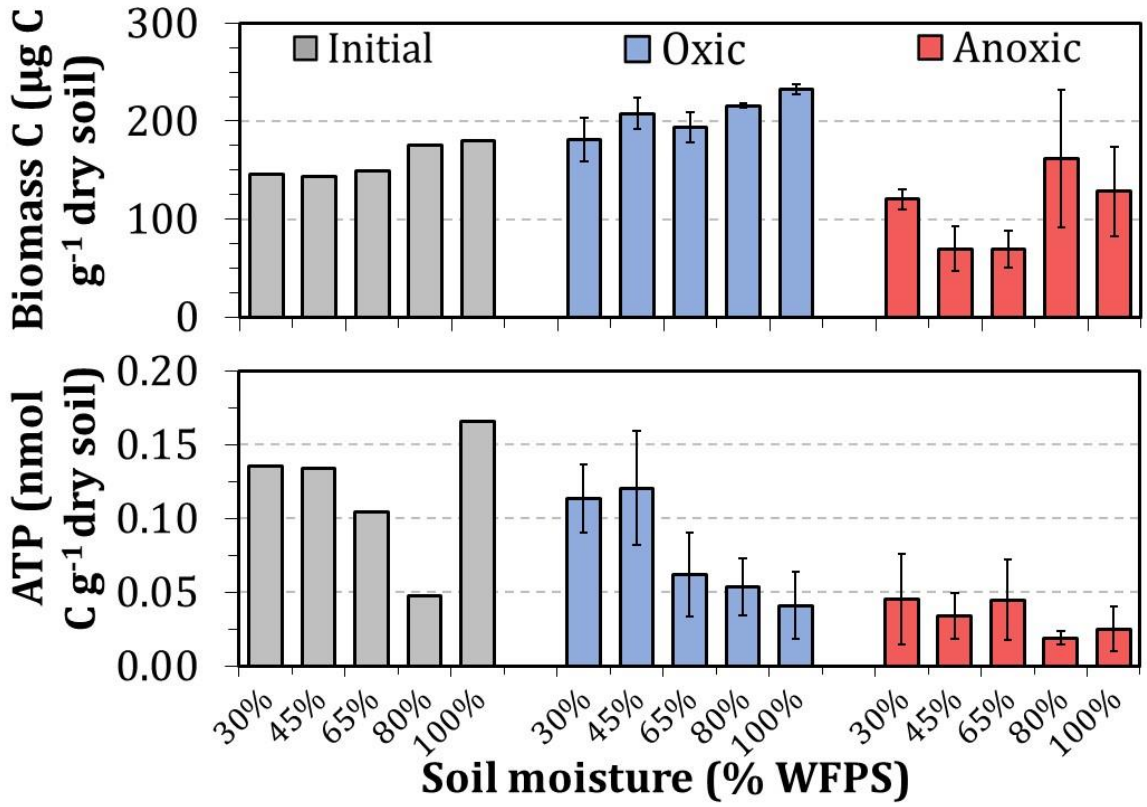

Figure A-4: Microbial biomass C (top) and soil ATP (bottom) measured at the beginning of the Chapter 2 experiment (initial – grey), and at the end of the incubation (oxic – blue; anoxic – red). Methods are briefly described in this appendix. Error bars represent standard deviation (n=3), not shown for initial measurements (n=1).

Additional materials and methods

Upon sacrificing the initial and final soil samples, duplicate subsamples (1.5-2.0 g bulk soil) were immediately prepared for analysis of soil biomass carbon (C) and nitrogen (N) via the chloroform fumigation extraction technique outlined in Vance *et al.* (1987). Both fumigated samples (24 hr chloroform fumigation in a vacuum desiccator) and non-fumigated samples were extracted with 0.5 M K_2SO_4 (1:4 soil-to-extractant ratio), centrifuged at 3500 rpm for 15 min and the supernatants filtered (0.45 µm polypropylene syringe filters, VWR). Filtered extracts were acidified with HCl to pH <2 and analyzed for DOC on a total organic carbon analyzer (Shimadzu TOC-LCPH/CPN). Biomass C was calculated as the difference between the extractable DOC concentrations of the fumigated and non-fumigated samples using an extraction factor of K_{ec} = 0.45 (Joergensen, 1996).

Additional subsamples of initial and final samples were also immediately flash frozen in liquid nitrogen and stored at -20°C for later analysis of adenosine triphosphate (ATP) concentration based on a method adapted from Jenkinson and Oades (1979) and Redmile-Gordon *et al.* (2011). Samples (0.6-1.0 g bulk soil) were extracted in the "TIP" reagent (0.92 M trichloroacetic acid, 0.59 M imidazole, 0.47 M Na_2HPO_4; 1:10 ratio). Samples were sonicated for 2 min, cooled on ice for 8 min, filtered (Whatman 42 filter), flash frozen in liquid nitrogen and stored at -20°C. Analysis of ATP concentration was performed using an assay kit (BacTiter-Glo Microbial Cell Viability Assay, Promega) by diluting the soil extracts in 20 mM HEPES buffer (in place of the arsenate buffer used by Jenkinson and Oades, 1979). Luminescence of samples, matrix-matched calibration standards and blanks (autoclaved soil) were measured in triplicate using white 96-well plates on a microplate reader (FlexStation 3 Multi-Mode Microplate Reader,

Molecular Devices). The detection limit for this method was determined to be 0.0005 nmol g^{-1} dry soil.